UNIVERSITÀ DEGLI STUDI DELLA TUSCIA

Università degli Studi della Tuscia di Viterbo
Dipartimento per la innovazione nei sistemi biologici, agroalimentari e forestali

Corso di Dottorato di Ricerca in
Scienze, tecnologie e biotecnologie per la sostenibilità- XXXIII ciclo

TITOLO TESI DI DOTTORATO DI RICERCA

Standardization of the Eddy Covariance Instruments and Methods: Needs, Evaluation and Optimization

Settore scientifico-disciplinare

s.s.d. AGR/05

ASSESTAMENTO FORESTALE E SELVICOLTURA

Tesi di dottorato di:

Dr. Sundas Shaukat

Firma: ____________

Supervisor:

Prof. Dario Papale

Firma: ____________

Ph.D. Coordinator:

Prof. Andrea Vannini

Firma: ____________

Co-Supervisor:

Dr. Simone Sabbatini

Firma: ____________

A.A. 2020/21

Table of contents

List of Symbols

x(t)	generic time series
$\bar{u}_{PF}$	mean horizontal wind speed of planar fit (m s^{-1})
M_{PF}	rotation matrix of planar fit
u	first horizontal component of wind speed (m s^{-1})
v	second horizontal component of wind speed (m s^{-1})
w	vertical component of wind speed (m s^{-1})
U	wind speed (m s^{-1})
λE	latent heat energy
λ	latent heat of vaporization of water
M_a	molecular weight of dry air
M_w	molecular weight of wet air
P	*a*tmospheric pressure

ABSTRACT

Eddy covariance approach is employed worldwide to measure fluxes. This valuable EC data is utilized by global and regional networks to investigate the interaction between atmosphere and ecosystems. The essential components of EC method are sonic anemometer and infra-red gas analyser. Today different sonic anemometers and gas analyzers are available based on different technologies and with different characteristics. These different options, together with different data processing strategies commonly used, are a source of uncertainty that may potentially affect comparability among sites. A possible strategy to deal with this source of uncertainties, especially among research infrastructures and networks of eddy covariance sites, is to standardize the technique in its different steps, from the sensor selection to the instrument's setup and the data processing.

The effect of standardization is analysed in this thesis and divided in two sections; first is based on data from setups working in parallel (15 sites) with the aim to check the uncertainty in calculated fluxes (CO_2, latent heat and sensible heat) due to different instrumental setups and processing methods on a large number of sites covering different climate and ecosystems where a standard setup (ICOS) is running in parallel to a nonstandard instrumentation. Second part is reprocessing of long-term data (9 sites) with the objective of understanding the effect of change in setups on a long timeseries, and to check whether a standardized processing may result in making the historical dataset collected with different instruments and processed in different ways more coherent. Results pointed out that the range of variability due to different instrumental setups, processing and methods of correction and filtering of EC data is site dependent and both setup and processing play role.

Variability due different setups in ICOS processing was 16 % in Fc, 11 % in LE flux and 7 % in H flux, in PIs processing it was 10 % in Fc, 19 % in LE and 5 % in H flux on average. Variability due to different processing methods for ICOS setup was 9 % in Fc, 14 % in LE and 10 % in H flux. For non ICOS setup average variability due different processing methods was 17 % for Fc, 16 % for LE and 12 % for H flux. As EC is very complex method, there is not a single factor explaining the variability and differences, both the instrumental setup and the processing play a role. In general, it has been found that, reprocessing of long-term data from non ICOS setup with standardized ICOS processing helps to make fluxes comparable with ICOS setup.

Key words: Standardization, eddy covariance, flux measurements, variability, standardized processing schemes.

1. INTRODUCTION

1.1 Importance of Fluxes

Fluxes measurements are important information that can be used to explore ecosystem and atmosphere interactions. They are significant as they are necessary component of mass conservation. Trace gas flux information is a helpful tool to estimate wellbeing and performance of ecosystem, as it evaluates balance of vegetation and soil, and ability of ecosystem to handle the external pressure and stress (Baldocchi, 2014). There are number of direct and indirect techniques to measure the exchange of mass, energy and gases between ecosystem and atmosphere, eddy covariance is one of them. The use of EC data has become increasingly widespread, now its study is not only used to understand the ecology and physiology of individual ecosystem (e.g., Reichstein et al., 2007; Law et al., 2002; Mahecha et al., 2010; Luyssaert et al., 2007; Besnard et al., 2018) but also in many other fields like formulation and authentication of modelling and remote sensing applications as base observations (e.g., Bonan et al., 2011; Friend et al., 2007; Williams et al., 2009; Balzarolo et al., 2014; Jung et al., 2020). As a result of the vast range of potential purposes of EC data, networks such as CarboEurope (Dolman et al., 2006 and Ameriflux (Novick et al., 2018) were established. Later, number of other networks formed for example AsiaFlux, OzFlux, LBA and ChinaFlux (Yamamoto et al., 2005; Beringer et al., 2016; Restrepo-Coupe et al., 2013; Yu et al., 2006) and FLUXNET (Papale, 2020).

1.2 Eddy Covariance (EC)

EC is micro meteorological technique used to calculate vertical turbulent fluxes of greenhouse gases (GHGs), energy and matter, between the atmosphere and biosphere (Aubinet et al., 2012). The fluxes are calculated at a point over the canopy, as the covariance between vertical wind speed and scalars, such as temperature and gas concentrations, measured by dedicated instrumentation. Hence a typical EC system consists of a three-dimensional ultrasonic anemometer and an infrared gas analyser sampling at high frequency (10-20 Hz) (Aubinet et al., 2003).

$F = \bar{\rho}_d \overline{w'c'}$ eq. 1.1 a

$H = \bar{\rho} C_P \overline{w'T'}$ eq. 1.1 b

$LE \equiv \lambda E = \lambda \frac{M_w/M_a}{\bar{P}} \overline{\rho d w'e'}$ eq. 1.1 c

Eq. 1.1a is the formula for flux of any gas of interest (s), such as CO_2, CH_4, N_2O, O_3, *etc*. it is defined as a covariance between instantaneous deviation in vertical wind speed (w') from the mean value ($\overline{w}$) and instantaneous deviation in gas concentration, mixing ratio (s'), from its mean value ($\bar{s}$), multiplied by mean air density (ρ_d). Sensible heat flux (eq. 1.1b) is equal to the mean air density multiplied by the covariance between deviations in instantaneous vertical wind speed (w) and temperature (T); conversion to energy units is accomplished by including the specific heat term. Flux of water vapor is expressed in energy units (W m^{-2}) and known as latent heat flux (eq. 1.1c) that is covariance between instantaneous deviation in vertical wind speed (w') and water vapour. Latent heat flux describes the energy used in the process of evaporation, transpiration, or evapotranspiration (G. Burba, 2013). Turbulent flux carried both low and high frequencies to deal with these fluctuations, the sampling frequency for eddy covariance data acquisition has rate of 10-20 Hz. (Rebmann et al., 2012).

There are some important assumptions at the basis of the EC method. For example, the EC method only measures the vertical turbulent component of a given exchange of energy or matter with the atmosphere, then it is assumed that the other forms of transport, like advection and storage, are negligible. Also, the EC technique is carried out by installing the EC system at a single point above the canopy, thereby assuming that the overall fetch is homogeneous and flat. The footprint, i.e., the area contributing most to the measured fluxes, is also assumed to lie within the ecosystem of interest.

Other examples include the assumption that the air density fluctuations that would lead to artificial changes in concentration, are negligible, and mean air flow and turbulence at the measurement point are not appreciably distorted by the installation structure or the instruments themselves. All these ideal conditions are rarely met in the real world, and for that reason measurements are prone to different types of bias that need to be prevented, minimized, or corrected out (G. Burba, 2013).

1.3 Eddy Covariance System

The core part of an eddy covariance system is the sonic anemometer and the infrared gas analyser (IRGA). Now a days several manufacturers provide different types of sonic anemometers and IRGAs.

1.3.1 Sonic Anemometer

A 3-dimensional sonic anemometer uses 3 pairs of transducers to measure the speed of sound for each pair. Three vector components of wind speed are then computed, and the vertical wind speed component (*w*) is used for the eddy covariance calculations. The three main types of physical arrangement of sonic anemometers most used in eddy covariance are omni-directional design with *u*, *v* and *w* components measured in the same physical space by non-orthogonal off-axis pairs of transducers (*e.g*., not at 90° to each other) e.g. Gill R3-50, R3-100 etc , wind master series ; non-omni-directional c-clamp design with *u*, *v* and *w* components measured in the same physical space by non-orthogonal pairs of transducers e.g. Gill HS-50, HS-100, metek uSonic3 class A, CSAT3 etc ; and c-clamp design with *u*, *v* and *w* components measured in the same or different physical spaces by orthogonal transducers, with *w* measured by a pair of vertically aligned transducers e.g. Thies ultrasonic 3D (G. Burba, 2013) .

1.3.2 Infrared Gas Analyser

The concentration of water vapour and CO_2 are measured by infrared gas analyzers. The IRGA is a differential analyser that estimates gas concentrations by comparing absorption of infra-red energy in a measurement chamber with the one in a reference, gas-free chamber (closed-path types), or by using a single chamber and comparing the behaviour at two different wavelengths (open-path types) (Aubinet et al., 2000). Closed-path types are characterised by an inlet tube taking the air to the measurement cell by means of a pump, while in open-path sensors the cell is exposed to the air and no pump is needed. Today, there are also intermediate versions between open- and closed-paths, often referred to as “enclosed path”, where a single cell is used but enclosed in case, and the air is collected by using a short tube. High-speed gas analyzers with response rates of 10 Hz or higher are utilized for measurements of eddy covariance fluxes. The choice between an open-path, enclosed, or closed-path design is largely a function of power availability and frequency of precipitation events.

Open path analyzers’ frequency losses are quite small and are primarily related to path averaging and spatial separation between the sonic and the open-path analyser. Flux calculations based on in-situ density measurement require significant density corrections. Precipitation events are the main cause of loss of data. Low-power remote sites with little precipitation but large fluxes would be good candidates for the open-path device. In addition, the open-path design is well-suited for measurements of fluxes of H_2O and other "sticky" gases.

Closed path gas analyzers require the sample air to be mechanically drawn to the sample cell by a high flow rate air pump, thus increasing system power requirements. The limiting factors in closed-path system are the capability of sonic anemometer to operate during precipitation events, and loss of signal due to tube attenuation. Grid-power sites with large amounts of precipitation that are focused on fluxes other than H_2O would be good candidates for the closed-path device.

Enclosed analyzers are designed to be used with short intake tubes and fast temperature and pressure measurements of the gas in the cell, thus reducing tube attenuation of gas and water vapor fluctuations, eliminating density corrections, and lowering power consumption, without incurring susceptibility to precipitation related data loss. The enclosed design is well suited for most types of sites and fluxes but will require more power than the open-path design (Burba, 2013). The IRGA types used in this study are closed path (LICOR LI-7000 and LI-6262), open path (LICOR LI-7500) and enclosed path (LICOR LI-7200).

1.4 Flux Calculations

To calculate the final flux, raw EC data necessarily pass-through different corrections and filtering processes due to instrumental limitations and the fact that assumptions of eddy covariance methods are not always met. These steps are explained for example in (Aubinet et al., 2012) or (Sabbatini et al., 2018) and mentioned as follows. Many quality tests must perform on the raw time series to filter out the inappropriate data to avoid irregular flux calculation. Series of corrections starts from despiking, that is accomplished to remove the large irregular deviation from an average signal. In 1997 Vickers and Mahrt, listed a series of tests that could be used to mark EC raw data. Taylor and Loescher, 2013 described another series of tests to detect EC data problems of bad timing. Next step is selection of average interval (AI) of flux. Most EC communities use 30 minutes as suitable AI (e.g., Aubinet et al., 2000), as AI must be long enough to accommodate large and slow eddies at a low-frequency spectrum and short enough to avoid including non-turbulent movements. Coordinate rotation correction is applied on sonic anemometer wind data to fulfil the basic assumption of EC method that on average no vertical motion is present ($w = 0$ averaged on AI). Therefore, the linking frame should be rotated so that the equilibrium vertical turbulent flux divergence is approximately the same as the total output flux divergence and as far as possible (Finnigan et al., 2003). Double rotation by Aubinet et al., 2000 and planar fit by Wilczak et al., 2001 are widely used methods in EC community for coordinate rotation. In double rotation coordinate rotation for each averaging period is performed, as a result mean cross wind and the vertical wind component become zero to meet EC assumption. Planar fit method executes different rotations for each of selected number of wind sectors on adequate long dataset. Regression coefficients are calculated by bilinear regression, these coefficients are used to drive rotation angle for each sector and angles can be used for all averaging periods.

Correction for the concentration/mole fraction is applied to solve the issue related to IRGA drift. Calculation of background signal and fluctuations are performed to separate background signals and fluctuations of the time series. Block average and linear detrending methods by Gash and Culf in 1996 are widely used for separation of fluctuations of the variables from background signals. In block average calculation of mean value of variable is followed by calculation of turbulence fluctuations as individual deviance from mean, whereas linear detrending is based on linear regression between time series and time and eliminates the linear trend that is present over the average interval.

Time lag compensation is another correction that is applied for removal the lag present between the measurement of vertical wind velocity and gas scalars from two instruments. Compensations of density fluctuations also known as WPL (Webb et al., 1980) is another step that includes the conversion of gas concentrations (mol m^{-3}) or mole fraction (mol mol_w^{-1}) into dry mole fraction (mol mol_d^{-1}). This compensation will not be applicable when output of IRGA is already in dry mole fraction, typical for closed and enclosed IRGAs where pressure, temperature and volume are controlled. Losses of flux due to high and low frequencies not detected by the sensors are compensated by spectral correction that at least partially correct also issues due to not perfect time response, tube attenuation, scalar and vector path averaging, sensor separation, sensor response mismatch, low and high pass filtering, and digital sampling (Burba 2013). Scientists proposed both analytical and in-situ methods for spectral correction, for example the one used in ICOS and proposed by Fratini et al., 2012 that has the characteristic of calculating spectral correction factors taking into consideration the relative humidity effect in the sampling line (important for water fluxes) and suggested for closed and enclosed path system with long sampling tube. Correction for the effect of humidity on the sonic temperature is also applied according to method proposed by (Schotanus et al,.1983 and by Van Dijk et al., 2004. After the fluxes calculation and the application of the corrections, quality check tests are performed on calculated fluxes for filtering bad quality data using data quality flags to produce clean timeseries of fluxes (described in the materials and methods section).

1.5 Eddy Covariance Networks

In the recent years there has been a remarkable increase in the number of eddy covariance (EC) monitoring sites and networks worldwide that use different sonic anemometers and gas analyzers based on different technologies and characteristics to measure the exchanges of gas, energy and water between a given surface and the atmosphere. Use of different sensors to collect high-frequency raw data, and different processing steps to convert raw data to half hourly fluxes, introduce different degrees of uncertainties that may alter the measurements and affect inter-comparability among sites, whose data are used to develop models and investigate several important scientific questions, for example by means of multi-site syntheses of flux data on the terrestrial carbon cycle.

As every step has some degree of uncertainty (e.g. because different methods are available), the final uncertainty of the EC method is the result of the combination of every single source of error. While several studies exist that characterize both the random and the systematic components of the errors in eddy covariance measurements (e.g. Finkelstein and Sims, 2001; Richardson et al., 2012; Loescher et al., 2006), the comparability of fluxes measured by different sites in different ecosystem using different models of sensors and processed by different software using different approaches is becoming more and more challenging with the number of EC sites and networks is growing worldwide, and something deserving attention and investigation. To deal with that, some EC monitoring networks are going towards higher degrees of standardization of setup and processing options, to reduce some systematic biases and hopefully increase inter-comparability of results. Their hypothesis is that standardization increases the inter-comparability of the calculated turbulent fluxes, while heterogeneous, non-standardized procedures are less comparable, likely adding more uncertainty. However, others give more importance to the diversification because each specific ecosystem condition could require a different solution. For example, three of the most important eddy covariance networks currently active at a continental or global scale, i.e., Ameriflux, ICOS (Integrated Carbon Observation System) and NEON (National Ecological Observatory Network), have different strategies in terms of sensors selection, setup, and processing methods, as summarised in **table 1**.

ICOS	NEON	AmeriFlux
Standardized EC setups, not standard meteo (WMO)	Standardized EC setups, Standardized meteo	EC setups checked centrally but not standardized
Standardized and centralized raw data processing	Standardized and centralized raw data processing	Processing decided and applied by sites PIs

Table 1 Rules for sensor selection, setups, and processing methods in ICOS, NEON and AmeriFlux. PI = Principal Investigator of the site

Then every network standardizes at a different pace and with different approaches, resulting in a variety of different instruments deployed and processing methods applied (including QA/QC) both within and between the networks. In the past years some efforts have been put in the standardization of the processing methodology, but many steps remains site- and instruments-specific, raising some concerns for the organization of the standardization (Mammarella et al., 2016).

All in all, it remains unknown the effect and possible improvement in fluxes comparability of the standardization effort applied to the eddy covariance technique. In particular open questions are 1) which part of standardization (setup, calculation, filtering) is more relevant or useful, if any? 2) What is the impact on the variability of calculated turbulent fluxes of standardizing vs non-standardizing? It must be also noted that inter-comparability is not only affecting the comparison between sites but is relevant also in terms of timeseries, at those sites measuring since many years (long-term sites hereafter), where instrumentation is regularly upgraded, and processing methods applied could be also not consistent. Interannual variability of eddy covariance fluxes at those sites can be impacted by a change in methodology and /or instrumentation.

1.6 Thesis Objectives

Hence, the present PhD thesis aims at investigating both the effect of setup and processing (calculation and filtering) standardization by using data from sites as part of the ICOS network running an EC system in addition to the ICOS standard ("parallel" study), and at understanding the effects of instruments upgrading and changes on long timeseries. Overall, this work will help to recognize what the standardization of sensors and methods weights in terms of improving comparability, and what is its contribution in terms of uncertainty. In the long-term study historical time series data were reprocessed for nine sites, as contribution to one of task of project RINGO (Readiness for ICOS Necessities of Integrated Global Observation: https://www.icos-ri.eu/ringo) in which PIs of the ICOS participated by sharing their raw EC datasets.

As shown above, sites part of ICOS must use a standard EC setup, composed by the same models of sonic anemometer and gas analyser (Sabbatini and Papale, 2018). Most of the currently ICOS sites, however, were existing since many years (up to 15) before entering in the ICOS network. This means that they produced historical dataset with non-standardized setup, processing, and software. These long-term data have an enormous value and have been used in many studies, models, and shared in large databases. When they entered ICOS, they had to conform to the network standard, then creating a discontinuity in the long-term dataset that it is important to understand how much is comparable with the current ICOS data collected.

To summarize, the main objectives of this activity are:

1) To examine the effect of standardization of instrumental setup and processing methods in term of uncertainty in calculated fluxes (CO_2, latent heat and sensible heat) using the parallel setups for the first time in a systematic way and on a large number of sites covering different climate and ecosystems.

2) Reprocessing of long timeseries aims at understanding the effect of change in instrumental setups, and to check whether a standardized processing may result in making the historical dataset collected with non-standardized instrumental setup more comparable with the present dataset and analyse the effect of the change in the instrumentation.

2. MATERIALS AND METHODS

The activity was performed in two sections: 1) parallel measurements and 2) Reprocessing of long-term data. The methods mentioned below were performed on both steps.

2.1 Data Collection

For the collection of raw EC data, several PIs (Principal Investigator of the site, leading the site team) of different ICOS sites within Europe (15 sites) were contacted for data sharing both for parallel measurements and reprocessing of long-term data. In ICOS, both the instrumental setup and the data processing methods are standardized; however, the PIs were often running their system since before, and some of them have periods of overlap between the ICOS (i.e. LICOR LI-7200 & Gill HS-50 or Gill HS-100) and a different system (i.e. closed path or open path IRGA and a different sonic model). PIs were requested to send raw EC data (acquisition frequency of 10 or 20Hz) along with the relevant metadata that contains all essential information related to IRGA and sonic anemometers, units of the variables, heights of instruments etc for correct processing of fluxes. Metadata were categorised in three groups: information on the file structure (file format, number of columns, variables in the files), information on the setup characteristics (single or parallel systems, brands and models of instruments used, instruments height and orientation etc.) and information on the ecosystem (ecosystem type, canopy height). The metadata was collected using the BADM (Biological, Ancillary, Disturbance and Metadata) system, a protocol for metadata collection standardized among different networks (ICOS, AmeriFlux, Fluxnet). Based on the metadata, homogeneous periods in terms of file structure are identified, and, an example file is asked for each period, to understand its exact content format and size. In addition, the team responsible for the site applied their own processing to both the systems and these data were also collected and compared with the ICOS ones.

Handling of metadata for long time series was very pivotal. The main issues found are the use of different formats (ASCII, several type of binary files) also in the same site and year, analog data without the parameters for conversion to physical units (lost and not found by the PIs), sensor diagnostics not recorded, incomplete or missing metadata (setup, maintenance and disturbance periods, processing applied) and unclear timestamps (beginning or end of averaging period, DST shift and Time zone used) that impacted the processing and possibly also the results.

2.2 Data Organization

After gathering all the necessary information, data were organized and grouped depending upon the homogeneity of file format, file duration, number, and order of columns. Eddy covariance metadata (ECMD) tables that summarize the significant information for the processing and can be imported by the processing software, were prepared using metadata of the relevant sites and any change related to acquisition frequency, instruments, instrument height and displacement, canopy height, units of the variables were reported with date and time. RFlux, that is R package for processing and cleaning eddy covariance flux measurements (developed by Vitale et al., 2020 in the context of the ICOS activities) is used in this activity.

For some sites EC raw data in binary file format were converted into ASCII file using the Campbell Scientific® Logger Net and LICOR® EddyPro software, to obtain a dataset ready to be processed with the RFlux. **Table 2** reports the description of the setups, software and processing methods used by PIs of the respective ICOS sites and applied by them to both the ICOS and the non-ICOS setups. **Table 3** reports the description of the setups, software and processing methods used by PIs of the respective ICOS sites for long-term data.

Common Features			*Non ICOS Setups and Processing*						
Sites	**Ecosystem**	**Duration (Months)**	**EC Setups**	**Software**	**Tube Length (cm)**	**Rotation Method**	**Detrending Method**	**Spectral Correction**	**QC Method**
DE-Geb	CRO	12	LI-7000 & R3	EddyPro	1285	DR	BA	Ibrom et al., 2007	Mauder and Foken, 2004
DE-Tha	ENF	12	LI-7000 & R3	EddyPro	6300	PF	BA	Fratini et al. 2012	Mauder and Foken, 2004
CZ-BK1	ENF	4	LI-7000 & R3	EddyPro	500	PF	BA	(Moncrieff et al., 1997) (non ICOS(Ibrom et al., 2007)(ICOS)	Mauder and Foken, 2004
BE-Lon	CRO	7	LI-7000 & R3	Eddysoft	1240	DR	BA	(Eugster & Senn, 1995)	Foken and Wichura 1996
FR-Pue	EBF	12	LI-6262 & R3	EddyPro	350	DR	BA	(Ibrom et al., 2007)	Mauder and Foken, 2004
SE-Svb	ENF	8	LI-7200 & METEK	EddyPro	71	DR	BA	(Ibrom et al., 2007)	Mauder and Foken, 2004
CH-Oe2	CRO	4	LI-7500 & HS-100	EddyPro	-	DR	BA	Fratini et al. 2012	-
FR-Fon	DBF	12	LI-7500 & R3	EddyPro	-	DR	BA	(Moncrieff et al., 1997)	Mauder and Foken, 2004
FR-Aur	CRO	12	LI-7500 & CSAT3	Edire	-	DR	-	-	(Thomas Foken et al., 2012) Aubinet, 2002
FR-Lam	CRO	12	LI-7500 & CSAT3	Edire	-	DR	BA	(Moore, 1986	Foken, 2004 Foken and Wichura, 1996 Göckede et al., 2008
IT-Ren	ENF	2	LI-7500 & HS-100	Eddysoft	-	DR	-	-	Clapeyron Clasius eq. Based method
CZ-Wet	WET	2	LI-7500 & R3	Edire	-	DR	BA	Moncrieff et al., 1997	Mauder and Foken, 2004
DE-RuS	CRO	7	LI-7500 & CSAT3	TK3	-	DR	BA	Moore, 1986	Mauder et al., 2013
FR-Bil	ENF	10	LI-7500 & R3	EddyPro	-	DR	BA	Moncrieff et al., 1997	Mauder and Foken, 2004
IT-Mbo	GRA	12	LI-7500 & R3	EddyPro	-	DR	BA	Moncrieff et al., 1997	Mauder and Foken, 2004

Table 2 reports the details of the sites, ecosystem, duration of data available. EC setups, software, tube length, methods of coordinate rotation, detrending, spectral correction and quality checks used by PIs of the respective ICOS sites. CRO=cropland, EBF= evergreen broadleaf forest, ENF= evergreen needle leaf forest, WET= wetland, GRA=grassland, DBF=deciduous broadleaf forest, DR=double rotation, BA=block average, PF=planar fit. LI-7200 is enclosed path, LI-7000 & LI-6262 is closed path and LI-7500 is open path IRGAs (infrared gas analyzer).

Common Features			*Non ICOS Setups and Processing*								
Sites	**Ecosy stem**	**Duration (Years)**	**IRGA-Type**	**EC Setups**	**Year of Change**	**Software**	**Tube Length (cm)**	**Rotation Method**	**Detrending Method**	**Spectral Correction**	**QC Method**
DE-Geb	CRO	12	Closed path	LI-7000 & R3	2017	EddyPro	1285	DR	BA	Ibrom et al., 2007	Mauder and Foken, 2004
DE-Tha	ENF	12	Closed path	LI-7000 & R3	2017	EddyPro	6300	PF	BA	Fratini et al. 2012	Mauder and Foken, 2004
CZ-BK1	ENF	4	Closed path	LI-7000 & R3	2012	Edire (till 2011) Eddypro	500	PF	BA	Moncrieff et al., 1997 (non ICOS) Ibrom et al., 2007 (ICOS)	Mauder and Foken, 2004
BE-Lon	CRO	7	Closed path	LI-7000 & R3	2014	Eddysoft	1240	DR	BA	Eugster and Senn, 1995	Foken and Wichura 1996
FR-Pue	EBF	12	Closed path	LI-6262 & R3	2014	EddyPro	350	DR	BA	Ibrom et al., 2007	Mauder and Foken, 2004
FI-Hyy	ENF	23	Closed path	LI-6262 & R2	2018	-	770	DR	BA	Mammarella et al., 2009	Mauder and Foken, 2004
FI-Sii	WET	13	Closed path	LI-7000 & METEK	2015	-	1300	DR	BA	Mammarella et al., 2009	Mauder and Foken, 2004
CZ-Wet	WET	2	Open path	LI-7500 & R3	2012	Edire (till 2011) Eddypro	-	DR	BA	Moncrieff et al., 1997	Mauder and Foken, 2004
FR-Bil	ENF	10	Open path	LI-7500 & R3	2015	EddyPro	-	DR	BA	Moncrieff et al., 1997	Mauder and Foken, 2004

Table 3 reports the details of the sites, ecosystem, duration of data available. IRGA type, EC setups, year of setup change, software, tube length, methods of coordinate rotation, detrending, spectral correction and quality checks used by PIs of the respective ICOS sites. CRO=cropland, EBF= evergreen broadleaf forest, ENF= evergreen needle leaf forest, WET= wetland, GRA=grassland, DBF=deciduous broadleaf forest, DR=double rotation, BA=block average, PF=planar fit)

2.3 4 Processing Schemes

Two methods of coordinate rotation and two methods for detrending were used in the centralized standard processing, as suggested in Sabbatini et al. 2018 and in the ICOS infrastructure, for a total of 4 processing schemes. Double rotation and planar fit method were selected for coordinate rotation correction and block average and linear detrending were opted for detrending.

2.4 Coordinate rotation

Double Rotation Method

In 2000 Aubinet et al. described that coordinate rotation for each averaging period is performed to make both the mean crosswind component ($\overline{v}$) and vertical wind component ($\overline{w}$) zero. With this rotation the mean wind speed *U* follows the direction of $\hat{\imath}$ (unit vector of cartesian coordinate system). This step meets the EC assumption i-e *w*=0. Coordinate frame is rotated prior to the mean horizontal wind is directed toward $\hat{\imath}$:

$$\begin{cases} \mathrm{u}_1 = \mathrm{u}_0 \cos\alpha + v_0 \sin\alpha, \\ v_1 = -\mathrm{u}_0\, sin\,\alpha + v_0 \cos\alpha, \\ \mathrm{w}_1 = \mathrm{w}_0 \end{cases}$$ eq. 3.3.1 a

where

$$\alpha = tan^{-1}\frac{\overline{v_0}}{\overline{u_0}}$$ eq. 3.3.1 b

averaged value over the AI is represented by overbar operator. The second rotation pushes the mean vertical wind to zero:

$$\begin{cases} \mathrm{u}_2 = \mathrm{u}_1 \cos\beta + w_1 \sin\beta, \\ v_2 = v_1\,, \\ \mathrm{w}_2 = -\,\mathrm{u}_1 \sin\beta + w_1 \cos\beta \end{cases}$$ eq. 3.3.1 c

where

$$\beta = tan^{-1}\frac{\overline{w_1}}{\overline{u_1}}$$ eq. 3.3.1 d

Planar Fit Method

This method is defined by Wilczak et al., 2001 and is best for long datasets, for specific number of winds sectors a different rotation is performed, using different algorithm that fits a plane to the unrotated wind dataset

$$\overline{w_0} = b_0 + b_1\,\overline{u_0} + b_2\,\overline{v_0}$$ eq. 3.3.2 a

where $\overline{w_0}$, $\overline{u_0}$ and $\overline{v_0}$ are time series of mean unrotated wind components and b_0, b_1 and b_2 are regression coefficients. Regression coefficients are calculated by bilinear regression, rotating the mean horizontal component in $\hat{\imath}$ ($\overline{u_{PF}}$) with a matrix M_{PF}: a1

$$M_{PF} = \begin{pmatrix} \cos\alpha & 0 & -\sin\alpha \\ 0 & 1 & 0 \\ \sin\alpha & 0 & \cos\alpha \end{pmatrix} = \begin{pmatrix} 1 & 0 & 0 \\ 0 & \cos\beta & \sin\beta \\ 0 & \sin\beta & \cos\beta \end{pmatrix} \quad \text{eq. 3.3.2 b}$$

where α and β are associated to $b1$ and $b2$:

$$\sin\alpha = \frac{-b_1}{\sqrt{b_1{}^2 + b_2{}^2 + 1}} \quad \text{eq. 3.3.2 c}$$

$$\sin\beta = \frac{b_2}{\sqrt{b_2{}^2 + 1}} \quad \text{eq. 3.3.2 d}$$

$$\cos\alpha = \frac{\sqrt{b_2{}^2 + 1}}{\sqrt{b_1{}^2 + b_2{}^2 + 1}} \quad \text{eq. 3.3.2 e}$$

$$\cos\beta = \frac{1}{\sqrt{b_2{}^2 + 1}} \quad \text{eq. 3.3.2 f}$$

These coefficients are used to drive rotation angle for each sector and angles can be used for all averaging periods. This rotation does not require for every averaging period and that can be adapted in a selected number of wind sectors. However, if the long-term mean vertical wind speed is zero, does not mean that the short term (length of AI) mean vertical wind is also zero. After performing rotation for coordinate frame with the long-term angles, for each selected period the mean horizontal wind speed must directed toward $\hat{\imath}$. Whenever sonic anemometer position is changed a new plane must be fixed.

2.5 Detrending

Block Average Method

Gash & Culf, 1996 described block average as calculation of mean value of variable, followed by calculation of turbulence fluctuations as individual deviance from mean, so that average $\bar{x}_{BA}$ is:

$$\bar{x}_{BA} = \frac{1}{N}\sum_{j=1}^{N} x_j \quad \text{eq. 3.3.3 a}$$

$$x_j{}'_{BA} = x_j - \bar{x}_{BA} \quad \text{eq. 3.3.3 b}$$

where N is the number of numerical sampling instants j of the time series $x(t)$ (discrete form) in the average interval. Block average meets Reynolds averaging conditions (Lee et al., 2004), due to constant mean in the averaging interval.

Linear Detrending Method

In 1996 Gash & Culf, described linear detrending as method to separate turbulent fluctuations from the background signal. linear detrending is based on linear regression between time series and time and eliminates the linear trend that is present over the average interval, that defined as the best linear fit over the period. The linear trend is presented as:

$$\overline{x_{LD}} = S * t + I \qquad \text{eq. 3.3.4 a}$$

where S and I are slope and intercept. The fluctuations are then calculated from:

$$x'_{j\,\mathrm{LD}} = x_j - \bar{x}_{\mathrm{LD}} \qquad \text{eq. 3.3.4 b}$$

In digitally sampled signals the least squares regression is used to apply the linear detrending: *S* and *I* therefore calculated as explained by Rannik and Vesala, 1999:

$$S = \frac{N\sum_{j=1}^{N} t_j x_j - \sum_{j=1}^{N} t_j \sum_{j=1}^{N} x_j}{N\sum_{j=1}^{N} t_j^2 - \left(\sum_{j=1}^{N} t_j\right)^2} \qquad \text{eq. 3.3.4 c}$$

$$I = \frac{\sum_{j=1}^{N} x_j - s\sum_{j=1}^{N} t_j}{N} \qquad \text{eq. 3.3.4 d}$$

However, j denotes the sampling instant (so that x_j is a record of the time series at time t_j, and $x_{j'}$ is the detrended record at $t\,j$), N the number of instants in the average interval ($AI=N*\Delta t$, $\Delta t=(t_{j+1}-t_j)$). $\overline{x_{LD}}$ denotes the linear trend. This method does not meet Reynolds averaging condition because the mean is not constant in it.

2.6 Data Processing

The High-Performance Computer system hosted in the ICOS Carbon Portal (ICOS data repository and computing facility installed at Lund University, Sweden) and Department for Innovation in Biological, Agri-Food and Forest Systems (DIBAF, University of Tuscia) were used for processing of raw EC data from parallel setups and long-term sites using RFlux. The processing included conversion of non ICOS raw EC data files to RFlux compliant files, test statistics of the quality control routines on raw data files described by Vitale et al., 2020 processing of raw EC data using LICOR® EddyPro software with application of standard updated processing protocol provided by ICOS (Sabbatini et al., 2018) to the full dataset of the parallel systems and long-term data. The procedure was the combination of four different processing schemes using two different methods for coordinate rotation and linear detrending (mentioned in **table 5**), while keeping constant all the other processing options. These four combinations were applied on both setups in the parallel experiment. Four half hourly fluxes timeseries are obtained as a product of the processing for each of the two setups that then were compared against each other and with the PIs processed fluxes (for both ICOS and non ICOS setups) obtained with their standard (and site specific) processing. All the correction and their methods used in EddyPro for processing of raw EC data from both ICOS and non ICOS setups are reported in **table 4**.

Corrections	Methods used in ICOS	Four Processing Schemes
Rotation method	Double rotation (Aubinet et al., 2000),	Double Rotation & Block Average Double Rotation & Linear Detrending
	Planar fit (Wilczak et al., 2001)	
Detrending	Block average (Gash and Culf, 1996)	Planar Fit & Block Average Planar Fit & Linear Detrending
	Linear detrending (Gash and Culf, 1996)	
Time lag	Covariance maximization with default	-
Compensation of density fluctuations (non ICOS setups)	WPL	-
Foot printing estimation	Kljun et al. 2014	-
Spectral correction for High pass filtering effect	Moncrieff et al. (2004)	-
Spectral correction for Low pass filtering effect	Fratini et al. (2012)	-
Quality check methods (on raw data)	Vitale et al (2020)	-
spike count/removal	Vicker & Mahrt 1997	-
Quality check on half hourly fluxes	Vitale et al (2020)	-

Table 4 Correction and their methods used in EddyPro Processing of EC data.

2.7 Quality Check Tests

Quality control checks were done following Vitale et al., 2020. Evidence of errors comes from sequences of quality tests (listed in **table 5**), each test is flag of severe systematic error (SevEr), weak systematic error (ModEr), or presence of no error (NoEr). This process included two steps demonstrated in **figure 1**. Fluxes that took over at least one SevEr statement were rejected, while fluxes that received no SevEr statements and any number of ModEr statements are maintained. In the second step, outlier detection procedure was applied to the flux data that received no SevEr statement and only flux data that received a ModEr statement and identified as outlier simultaneously were removed. See Vitale et al., 2020 for more details on the tests applied and on the general strategy of data cleaning. **Table 5** summarizes the set of tests used in the data-cleaning process for this activity.

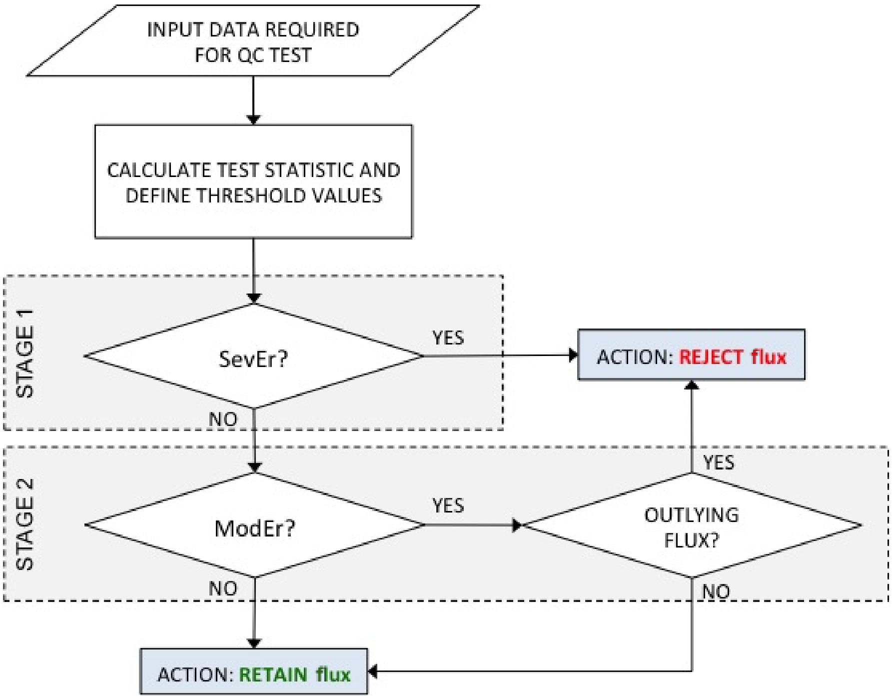

Figure 1 Schematic summary of the proposed data cleaning procedure by Vitale et al., 2020.

Sources of Errors	Tests Statistics	Threshold Values		
		NoEr	**ModEr**	**SevEr**
1- EC system malfunction and Disturbances	Fraction of missing records (FMR, %)	≤5	≤15	>15
	Longest gap duration (LGD, s)	≤90	≤180	>180
2- Low signal resolution	R^2 for linear regression of CCFs estimated with original data and after removal of repeated contiguous values	>0.995	≤0.995	<0.99
3- Aberrant structural changes (e.g. sudden shift in mean, changes in variance)	**a- Homogeneity test of fluctuations:**			
	HF5 – percent of fluctuations beyond ±5σ	≤2	≤4	>4
	HF1 – percent of fluctuations beyond ±10σ	≤0.5	≤1	>1
	b- Homogeneity test of differenced data:			
	HD5 – percent of differenced data beyond ±5σ	≤2	≤4	>4
	HD1 – percent of differenced data beyond ±10σ	≤0.5	≤1	>1
	KID – kurtosis index of differenced data	≤30	≤50	>50
4- Poorly developed turbulence regimes	Integral turbulence characteristics (%) by Foken and Wichura (1996)	≤30	≤100	>100
5- non-stationary conditions	Non-stationary ratio by Mahrt (1998)	≤2	≤3	>3

Table 5 Sources of systematic error, test statistics and adopted threshold values to define NoEr, ModEr and SevEr statements by Vitale et al., 2020.

2.8 Data Analysis

All the sites included in the parallel setup measurements and long-term data reprocessing have different time duration of raw EC data. Although all the available raw data were processed, but then to simplify the interpretation of results, only the calculated fluxes from three months of the growing season were used in analysis for all the sites except for CZ-Wet that has only two months of parallel measurements. Since data filtering and gaps are not randomly distributed and can be substantially different between sensors and processing schemes, comparing daily averages can be risky because, could be represented by different percentages of daytime and nigh time data. To solve this problem three months were divided in to 6 subsets (each of 15 days, in case of CZ-Wet 6 subsets were made from two months data and each subset has 10 days) for each of the 6 period, a median diurnal cycle was calculated. Each subset now has 48 half hours values available for the specific setup/processing. In this way 6*48 median values where obtained.

In ICOS and PIs processing different Qc methods were applied to the fluxes that resulted in data filtering. Percentage of data filtering is noticeably different between fluxes from different setups and processing schemes. Sites that have 40 % of data survived after Qc filtering for both setups (processed by ICOS and PI schemes) were used in the analysis. Available data percentages for all the sites of both parallel and long-term datasets are in appendices.

First analysis was performed by calculating averages of the median diurnal cycles (MDC) of six subsets of 4 processing schemes for all the site that survived the threshold for each flux. For the comparison of the same period half hour that is missing in one processing scheme was removed from rest of the results of the processing including PIs processing. Aim of this analysis is to compare results of 4 processing schemes of ICOS with coordinate rotation and detrending methods performed for ICOS and non ICOS setups to distinguish which processing weighs more. Results of PI processing that are obtained by using only one method of coordinate rotation and detrending for both setups were also compared with the range of variability made by 4 ICOS processing scheme to understand how much results vary from each other.

For further examination on the effect of standardization of setup, reduced major axis regression (RMA) model was applied to account the errors in both x and y variables. Variation in the fluxes from different setups and processing methods were quantified by using slope and R^2. Slope represented bias in proportion of flux magnitude and R^2 represented goodness of fit of the model. Average magnitude of the error between the fluxes from different setups and processing schemes was assessed by mean absolute error (MAE). Only one out of four processing schemes, the most like the one used by PIs of the respective sites was used to compare the results from two different setups processed by using ICOS strategy and PIs processing methods.

To evaluate the differences in processing methods RMA regression model was applied between results of ICOS and PIs (on MDC) processing methods for both ICOS and non ICOS setups. Processing includes both calculation and filtering, to compare the results of different processing methods, final fluxes (including both calculation and filtering due to quality check methods) were used. For the estimation of effect of quality check methods, RMA regression was applied on common half hours from the results of ICOS and PIs processing. Results were elaborated using slope, R^2 and MAE.

Percentages of data cleaning by ICOS and PIs quality check methods were calculated to know which method is filtering more and how much data is filtered in common by both methods. This analysis was only performed on fluxes obtained from ICOS setups to remove the effect of the different sensor behaviour and possible malfunctioning that are minimized in ICOS. These percentages were calculated by dividing number of half hours discarded from number of half hours expected in three months multiplied by hundred for all sites except CZ-Wet (two months data available). Additionally, percentages of data filtered by group of tests applied in ICOS quality check method were also calculated to discover which test is discarding more data.

Analysis of the long-term data followed a scheme like the one applied to the parallel setups, working on averages of the MDC of six subsets in the three months of growing season of each year for all the sites. Results of long timeseries were compared to estimate the interannual variability, difference in the fluxes due to two processing methods and change of setups. Boxplots were made to check the overall effect of different setups and different processing methods, with and without quality check filtering for parallel measurements.

3. RESULTS

3.1 Parallel Measurements (Site wise comparison)

The first activity is based on the results obtained from two different instrumental setups (referred as “setup”) working in parallel at the sites. Results are presented, separately for the three fluxes, in subsection to show: differences due to the four processing schemes, applied to both ICOS and non ICOS setups. In this analysis also the PIs results (calculated by using one method for coordinate rotation and detrending) were compared with results of four processing schemes with the aim to evaluate if the PI version was in the range of variability of the 4 ICOS versions. Fluxes obtained by two different setups and processed by using ICOS and PIs strategies were compared to understand the importance of instrument standardization. Fluxes obtained from different processing strategies for ICOS and non ICOS setups were compared for estimation of differences in two processing strategies, also separating the calculation and the filtering components of the processing.

3.1.2 CO_2 Flux (Fc)

For Fc thirteen out of fifteen sites were used in the analysis. In FR- Pue and FR- Fon filtering of Fc was more than 60 % of the data available.

3.1.2.1 Effect of 4 - Processing on Fc

In **figure 2**, averages of Fc are shown. Averages are calculated from MDC of Fc from growing season of thirteen sites. Plot represents three comparisons, that are 1) among Fc obtained from four processing schemes for ICOS setup (red dots), 2) among results obtained from four processing schemes for non ICOS setup (cyan dots), and 3) between the results of four processing schemes and PIs for both ICOS (red square) and non ICOS (cyan square) setups. Models of sonic anemometers working in setups are mentioned at the bottom of the plot while for the IRGA model refer to Figure 3. The four processing schemes defined the variability due to processing options used in each setup. Results demonstrated that Fc calculated from four processing do not vary much with in the same setup. Range of variability with in ICOS setup is 0.03 to 1.11 µmol CO_2m^{-2} s^{-1} and for non ICOS setup is 0.1 to 0.91 µmol CO_2m^{-2} s^{-1}. On average difference observed among four processing for ICOS setup is 0.3 µmol CO_2m^{-2} s^{-1} and 0.2 µmol CO_2m^{-2} s^{-1} for non ICOS setup.

Range of variability of Fc processed by using ICOS strategy applied to both ICOS and non ICOS setup is slightly larger at BE-Lon, SE-Svb, CH-Oe2, FR-Aur and FR-Bil where differences are in the order of 0.5-1 µmol CO_2m^{-2} s^{-1} while for the other sites the differences among the four processing options are minor. Fc calculated by PI and obtained from ICOS setup fall in the range of Fc obtained from the 4 ICOS processing schemes at DE-Tha, CZ-Bk1, FR-Aur, IT-Ren, DE-RuS and FR-Bil; in the other sites the differences are in the range 0.4 -1.8 µmol CO_2m^{-2} s^{-1}. A similar result is obtained comparing the PI version of the non ICOS setups, that fall in the range of the four ICOS processed Fc at SE-Svb, FR-Aur, IT-Ren, DE-

RuS, FR-Bil and IT-Mbo, with the rest of the sites showing differences of 0.6 -3 µmol CO_2m^{-2} s^{-1} (with FR-Lam the one with largest difference).

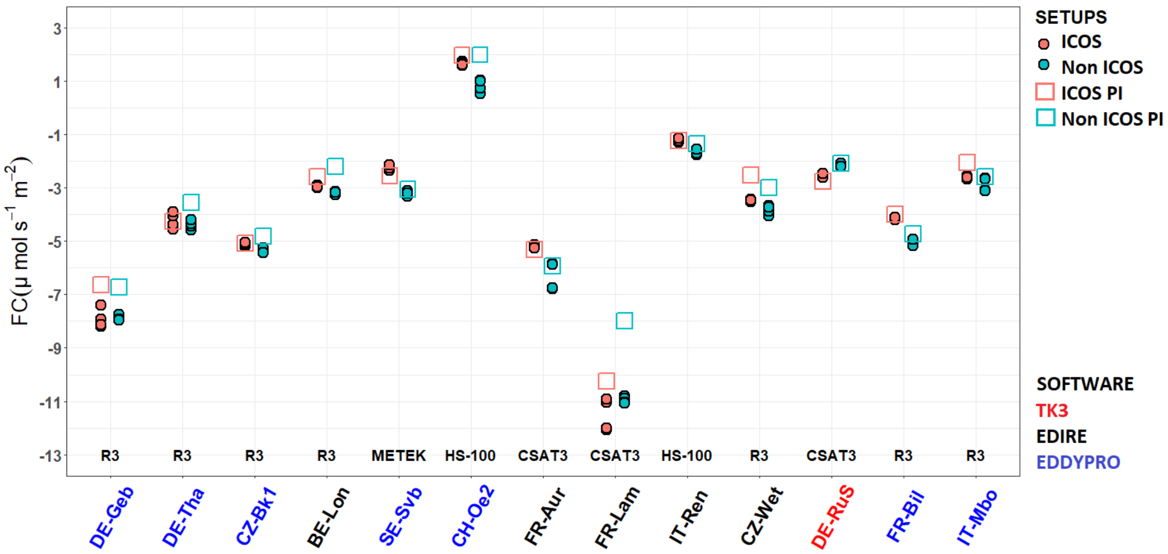

Figure 2 Averages of MDC of Fc for three months of growing season. Red represents ICOS setup and cyan represents non ICOS setup. Circles represents fluxes calculated by ICOS processing; square represents fluxes calculated by PIs. Four circles represent four processing schemes. Different colors of the labels of x-axis represent software used by PIs for flux calculations. Models of the sonic anemometers used in the non ICOS setups are mentioned at the base while for IRGA refer to figure 3.

RMA regression model was applied for further evaluation of the effect of different setups and different processing on Fc. In this case results obtained by only one out of four processing schemes was used in the next steps selecting the one using coordinate rotation and detrending as similar as possible to the one used by PIs. DR and BA were mainly applied at all the sites except CZ-Bk1 and DE-Tha where PF and BA were used.

3.1.2.2 Effect of Different Setups on Fc

In this part of the analysis, differences in fluxes due to a different setup, processed in the same way, was analyzed. Comparison between slopes for Fc calculated using ICOS processing and PI processing for both setups are demonstrated in **figure 3**. Slopes are calculated by applying RMA regression on Fc measured by ICOS setups (always on x axis) and non ICOS setup (on y axis), for both the processing schemes. Value of slope less than 1 shows that ICOS setup calculating higher fluxes. Filled circles are representing the slopes and mean absolute error (MAE) between Fc obtained using ICOS processing methods. Blank circles are representing the same but considering the processing applied by the PIs. Size of the circle (panel 1) is showing goodness of fit (R^2). Different colors of the circles are based on the technology of the IRGA.

In ICOS processing slopes between the two setups when the non-ICOS IRGA is a closed path are in general around 1, with R^2 more than 0.88, showing a good agreement and a small effect of the setup although must be also considered that all the 4 sites use a Gill R3 sonic. Sites using an open path IRGA the situation is more heterogeneous, and the slopes are significantly different from 1 (with exception of DE-RuS), in general larger (except FR-Lam). SE-Svb is the only site where the IRGA is the same used in ICOS but has a Metek sonic and reported high slope, with difference of 36 % ($R^2 = 0.93$) between the two fluxes.

In PI processing slopes for comparison of ICOS setup and non ICOS setups with closed path IRGA are smaller than 1, with R^2 more than 0.87. For PI processing SE-Svb is demonstrating difference of 12 % ($R^2 = 0.97$) between the Fc obtain from same IRGA type pairing with two different sonics, with the slope higher than 1; these large differences respect to the results obtained by the ICOS processing could be due to different treatment of the sonic data. In PI version of processing slopes calculated from regressing between ICOS setup and non ICOS setups with open path IRGA are smaller than 1 at CH-Oe2, FR-Lam CZ-Wet and DE-RuS.

In general, and to summarize, difference observed between the fluxes calculated from the raw EC data two setups is 16 % for ICOS and 10% for PI processing on average. It ranges between 2 % to 41 % for ICOS and 2 % to 23 % for PI processed results. In ICOS processing R^2 ranges between 0.66 to 0.98 among different sites, whereas in PI processing R^2 ranges between 0.87 to 0.98. For ICOS, it is also important to consider that the quality check filtering used removed a larger number of data resulting in smaller R^2 (see next sections). MAE between Fc obtained from two different setups varied between 1 and 5 µmol $CO_2 m^{-2} s^{-1}$ and 0.7-3 µmol $CO_2 m^{-2} s^{-1}$ for ICOS and PI processing schemes. On the whole, ICOS processing scheme indicated high mean absolute error for all the sites (except DE-Tha and FR-Lam) with the average of 2 µmol $CO_2 m^{-2} s^{-1}$ than PIs processing that is 1.3 µmol $CO_2 m^{-2} s^{-1}$.

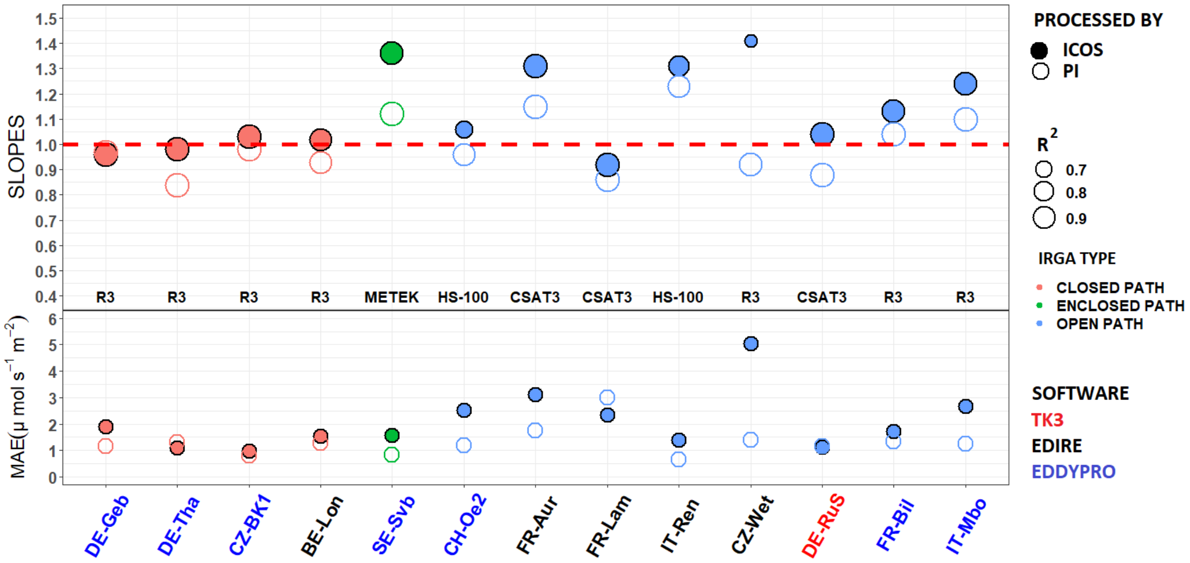

Figure 3 Effect of different setups on Fc. Panel 1: Filled circles represent the slopes obtained from RMA regression between fluxes from two different (ICOS and non ICOS) setups using ICOS standard processing scheme, blank circles represent the slopes obtained from RMA regression between fluxes calculated by processing made by the site PI from ICOS and non ICOS setups. Size of the circle represents R^2. Red, green and blue colours represent closed, enclosed and open path IRGA for non ICOS setups. Red dashed line represents the 1:1 reference (slope=1). Different colors of the labels of x-axis represent software used by PIs for flux calculations. Models of the sonic anemometers used in the non ICOS setups are mentioned at the base. Panel 2: Filled circles represent the MAE between fluxes from ICOS and non ICOS setups processed using ICOS standard processing scheme and blank circles represent the MAE between fluxes calculated by processing made by the site PI from ICOS and non ICOS setups.

3.1.2.3 Effect of Different Processing on Fc

This part of analysis was focused on the evaluation of differences in the final fluxes due to processing methods. Processing of the fluxes include calculation of the fluxes as well as the filtering done by quality check methods so in this case the differences are a combination of both the aspects. Comparison between slopes for Fc calculated using raw EC data from ICOS setup and non ICOS setup are demonstrated in **figure 4**. Slopes are calculated by applying RMA regression on the fluxes calculated by ICOS processing (on X axis) and PI processing (on Y axis), for ICOS setup and the non ICOS setup running in parallel at the selected sites. Filled circles are relative to the ICOS setup, blank circles to the non ICOS setup. Size of the circles represents value of R^2. Different colors of the circles are based on the technology of the IRGA.

Statistical analysis for ICOS setup resulted in slopes closer to 1 as compared with non ICOS setup for both closed path and open path IRGA types, highlighting a better correspondence between the PI and the centralized processing, with differences from reference line ranging from 1 % to 18 % (R^2 between 0.77 to 0.99) as compared to slopes calculated for non ICOS setup that are 5 % to 46 % (R^2 between 0.72 to 0.99). For both ICOS and non ICOS setups, higher values of Fc were however recorded for ICOS processing methods as compared to PI processing except for DE-Tha, SE-Svb, FR-Bil and IT-Mbo (ICOS setup). Fc calculated by ICOS setup and non ICOS setup at DE-Geb has almost same difference with respect to slope 1 although processed by different methods. Average percentage of variation is 9 % for ICOS and 17 % for non ICOS. SE-Svb is showing exceptional behavior with the difference of 10 % with R^2 of 0.98 and 0.95 between the fluxes calculated by ICOS and PI processing for ICOS and non ICOS setup (LI-7200+metek). As LI-7200 is used in this setup the processing methods and model of sonic anemometer are resulting the differences in the fluxes. Site with highest difference for non ICOS setup is CZ-Wet showed the differences more than 46 % with R^2 of 0.85. MAE between two different processing for ICOS setup is 1.8 µmol $CO_2 m^{-2} s^{-1}$ and for non ICOS setup is 2 µmol $CO_2 m^{-2} s^{-1}$ on average. Range of error between two processing for ICOS setup is 0.6 – 2.5 µmol $CO_2 m^{-2} s^{-1}$ and 0.8 – 5.5 µmol $CO_2 m^{-2} s^{-1}$ for ICOS and non ICOS setups. Fc obtained from ICOS setups has smaller values of MAE as compared to non ICOS setup with exception of DE-Tha.

It is worth to note that although EddyPro was used by several PIs (and this is the same software used in the ICOS processing), there seems to not be a clear software effect in the differences (colours of the station codes in **figure 4**).

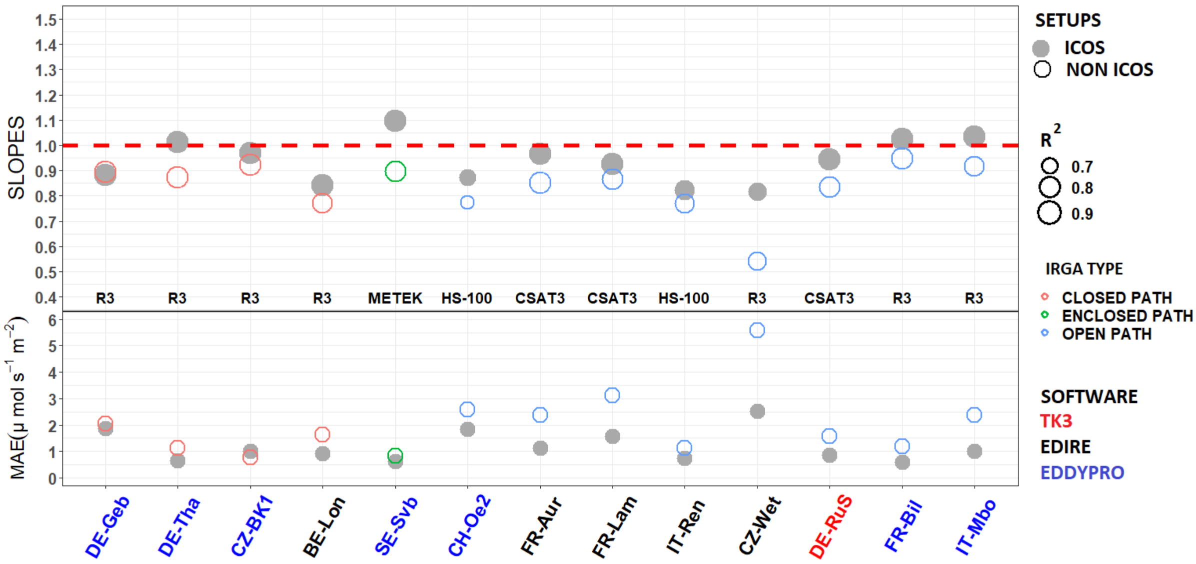

Figure 4 Effect of different processing schemes on Fc including both calculation and filtering by Qc. Panel 1: Filled circles represent the slopes obtained from RMA regression between fluxes from ICOS and PIs processing schemes, using ICOS setup. Blank circles represent the slopes obtained from RMA regression between fluxes from ICOS and PIs processing schemes, using non ICOS setup. Size of the circle represents R^2. Red, green and blue colours represent closed, enclosed and open path IRGA non ICOS setups. Red dashed line is the 1:1 reference

(slope=1). Different colors of the labels of x-axis represent software used by PIs for flux calculations. Models of the sonic anemometers used in the non ICOS setups are mentioned at the base. Panel 2: Filled circles represent the MAE between fluxes from ICOS and PI processing schemes using ICOS setup and blank circles represent the MAE between fluxes from non ICOS setup processed by PIs.

3.1.2.4 Differences in fluxes calculation (no filtering) on Fc

The previous analysis shows the differences due to the combination of fluxes calculation and filtering. To disentangle the two, the differences due to only calculation have been calculated. **Figure 5** demonstrated the coefficients of RMA regression of Fc calculated by using only common half hours that survived the respective data cleaning methods, for ICOS and non ICOS setups (and ICOS and PI processing). It is clearly observed from the results that slopes of ICOS setup are closer to 1 as compared to non ICOS setup. Removal of filtering effect reduced the variation between Fc processed by ICOS and PI by average of 3% for both ICOS and non ICOS setups. Slopes calculated from regression of Fc processed by ICOS strategy and PI for ICOS setup demonstrated smaller differences from reference line ranging from 1 % to 14 % as compared to slopes calculated for non ICOS setup that are 3 % to 40 %. Differences are 6% for ICOS and 14 % for non ICOS setup on average without the filtering process. R^2 for ICOS setup is between 0.97 to 1 whereas for non ICOS setup it is between 0.94 to 1. Likewise, the previous analysis (**figure 4**) ICOS setup has smaller MAE of 0.6 µmol CO_2m^{-2} s^{-1} in relation to non ICOS setup i-e 1.5 µmol CO_2m^{-2} s^{-1} on average. Range of error lies between 0.1 – 1.2 and 0.7 – 4.5 µmol CO_2m^{-2} s^{-1} for ICOS and non ICOS setups. It is observed that difference between the MAE and slopes of ICOS and non ICOS setup is reduced when the RMA regression is applied only on calculations without considering the filtration of Fc done by Qc (**figure 4**).

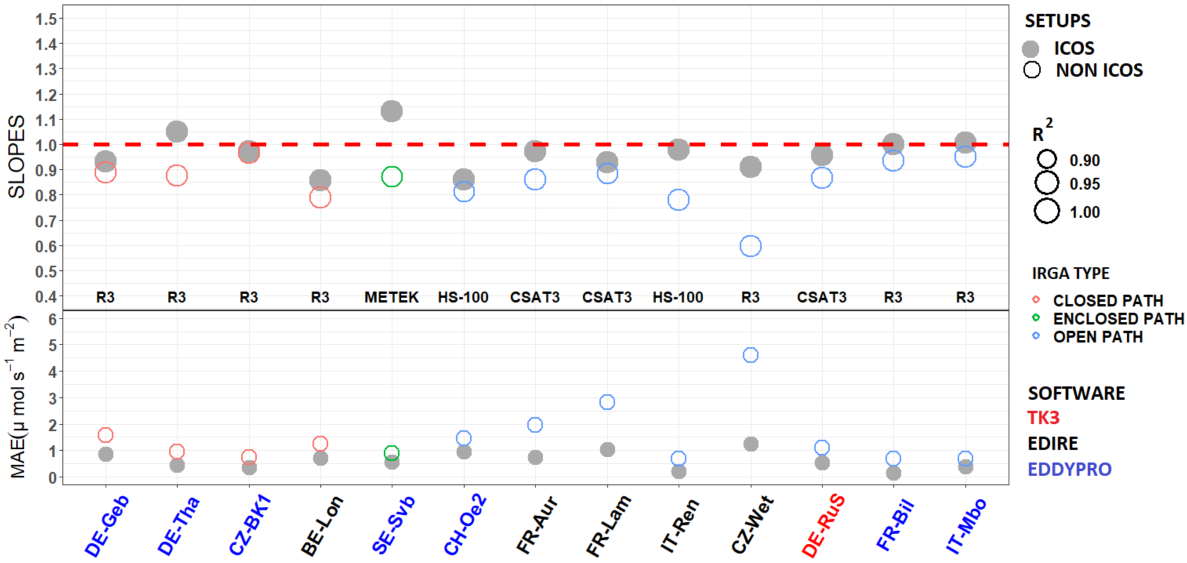

Figure 5 Effect of different processing schemes on Fc (calculation only). Panel 1: Filled circles represent the slopes obtained from RMA regression between fluxes from ICOS and PIs processing schemes, using ICOS setup. Blank circles represent the slopes obtained from RMA regression between fluxes from ICOS and PIs processing schemes, using non ICOS setup. Size of the circle represents R^2. Red, green and blue colours represent closed, enclosed and open path IRGA non ICOS setups. Red dashed line is the 1:1 reference (slope=1). Different colors of the labels of x-axis represent software used by PIs for flux calculations. Models of the sonic anemometers used in the non ICOS setups are mentioned at the base. Panel 2: Filled circles represent the MAE between fluxes from ICOS and PI processing schemes using ICOS setup and blank circles represent the MAE between fluxes from non ICOS setup processed by PIs.

3.1.2.5 Fc Filtered by ICOS and PIs Qc methods

Final fluxes derived from processing of raw data and processing comprised of calculation and data cleaning. On data processed by ICOS strategy, ICOS standard quality check tests were applied on all the sites to remove bad quality data, whereas in PIs processing quality check methods vary among sites (see materials and methods table 2). This part of analysis is only done on the results from ICOS setup for all the fluxes because all the sites are shifted to ICOS setup now. The effect of the filtering can be consistent and larger than what found in the previous section, where basing all on median fluxes single differences can be partially hidden. Quality check applied by ICOS consists of number of statistical tests (see material and methods table 5) that resulted in removal of bad quality data from all the sites. The same is done by the PIs that however apply a set of different filtering methods, often not documents and that can include a manual and visual filtering or even footprint. **Figure 6** showed percentage of the amount of data filtered. Percentages were calculated by dividing number of half hours discarded from number of half hours expected in three months multiplied by hundred for all sites except CZ-Wet (two months data available). Fc filtered by Qc ranges from 15 % to 66 % processed by ICOS and 7 % to 46 % processed by PIs across the sites involved in this analysis.

At DE-RuS and FR-Bil, PIs quality check methods are filtering more as compared to ICOS and these are the only two cases in the set used. Removal of bad quality flux concurrently by both ICOS and PIs quality check tests range from 5 % to 41 %. Maximum percentage of Fc filtration by both ICOS and PI is observed at FR-Pue where 41 % flux is removed during Qc filtering. For ICOS processing maximum data filtration is 66 % at IT- Ren and for PIs processing maximum removal of bad quality data is 46 % at DE-RuS. ICOS Qc method filtered more data as compared to PIs Qc methods because it included series of test statistics plotted in **figure 7.** Variation in percentage of data filtering among sites is due to different sources of error on individual site.

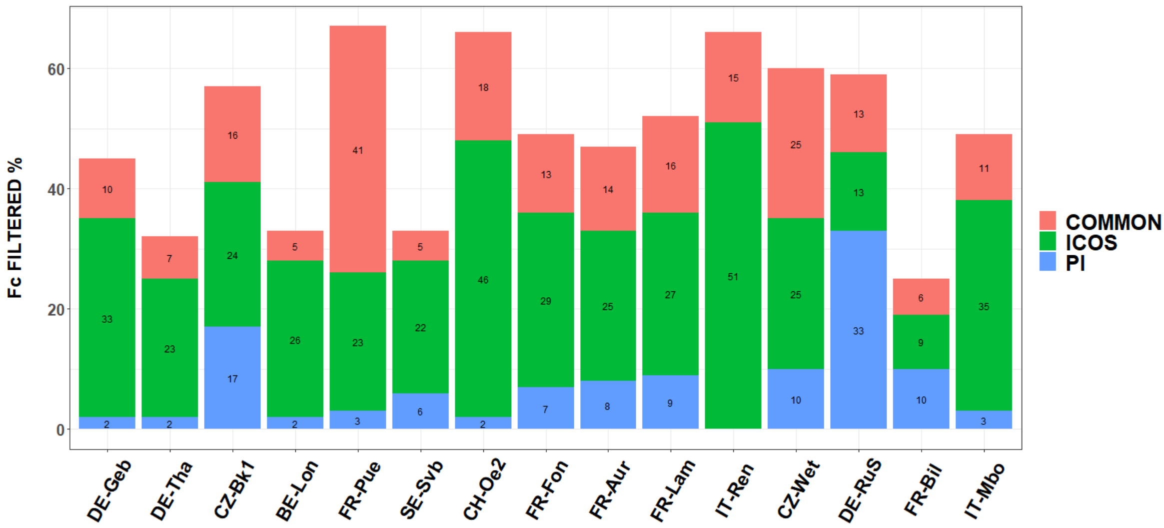

Figure 6 Percentage of Fc filtered by PIs, ICOS and both simultaneously. Red colour represents percentage of Fc filtered by both ICOS and PI, green colour represents percentage of Fc filtered by ICOS only and blue colour represents Fc filtered by PI only.

ICOS cleaning methods are based on Vitale et al., 2020 and consists of five main sources of errors (test statistics in table 5). Aberrant structural changes (ASC), EC system malfunction and disturbances (EC_sys_malf), integral turbulence characteristics (ITC), low signal resolution and non-stationary ratio by Mahrt (1998) (M98) are check for their thresholds during Qc filtering of fluxes at ICOS. **Figure 7** demonstrated the percentage of the Fc filtered due to above mentioned sources of error for ICOS setup processed by ICOS methods. Integral turbulence characteristics filtered minimum percentage of Fc whereas EC system malfunction and disturbances filtered maximum percentage of Fc across different sites for ICOS setup. Aberrant structural changes filtered 0 % to 40 %, EC system malfunction and disturbances filtered 0 % to 42 %, integral turbulence characteristics filtered 0 % to 1 %, low signal resolution filtered 0% to 13%, and non-stationary ratio by Mahrt (1998) filtered 11 % to 37 % Fc.

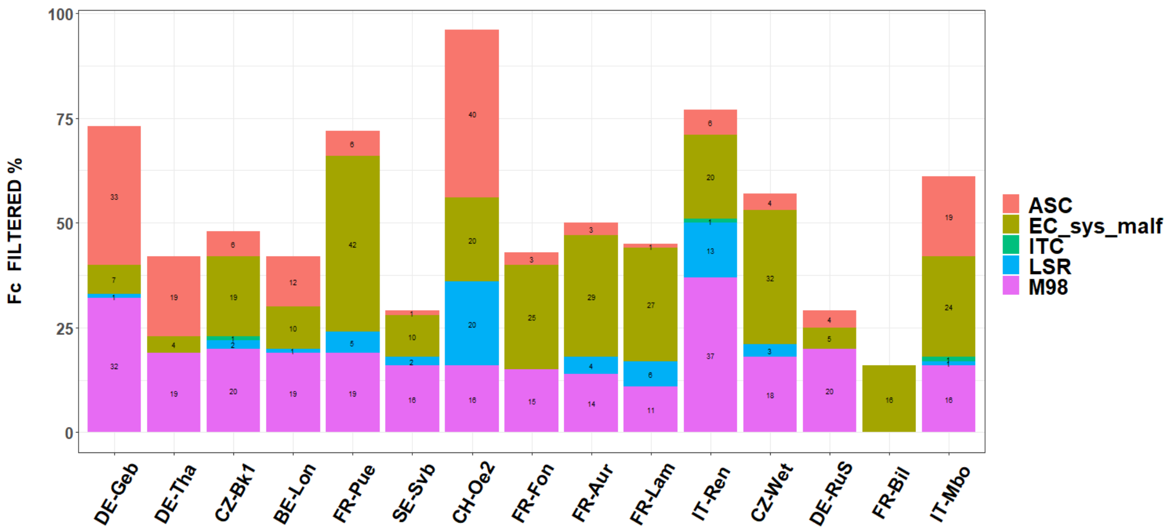

Figure 7 Percentage of data filtration for Fc by quality control tests applied at ICOS. Different colours represent five different sources of error as classified in the original paper of Vitale at al., 2020.

3.1.3 Latent Heat Flux (LE)

Ten out of fifteen sites were used in the analysis of latent heat flux. BE-Lon, FR-Pue, FR-Lam, FR-Fon and IT-Ren were not included because of data filtering more than 60 %.

3.1.3.1 Effect of 4 - Processing Schemes on LE Flux

Results indicated in **figure 8** that LE flux calculated from four processing varied with in the same setup at some sites. Fluxes from ICOS setup, calculated from four combination of correction methods for coordinate rotation and detrending varies from 0.1 to 33 W m $^{-2}$ with average variation of 6.4 W m $^{-2}$, while LE flux from non ICOS setup ranges from 0.1 to 24 W $^{-1}$m $^{-2}$ with average variation of 6.8 W m $^{-2}$. Minimum difference between LE fluxes obtained from ICOS and non ICOS setups processed by ICOS strategy is approximately 2 W m $^{-2}$ at DE-Tha and it goes up to 29 W m $^{-2}$ at CZ-Wet. The difference between average LE flux obtained from ICOS and non ICOS setup processed by PI ranged between 2 W m $^{-2}$ at DE-Geb and 42 W m $^{-2}$ at FR-Aur.

Average of LE flux obtained from ICOS setup and processed by PIs falls in the range of average LE flux of ICOS setup processed by using ICOS strategy at only at DE-Geb, DE-Tha, SE-Svb and FR-Bil. Rest of the sites demonstrated the difference ranged between 4 W m $^{-2}$ at CZ-Wet to 50 W m $^{-2}$ at FR-Aur of the situation is similar in the non ICOS setups where PIs processing results fall in the range of variability from four processing schemes only at DE-Tha, CZ-Bk1 and FR-Aur. For non ICOS setup minimum difference between PI processed fluxes and fluxes from ICOS processing methods is observed in IT-Mbo that is 7 W m^{-2} and maximum is 32 W m^{-2} at CZ-Wet.

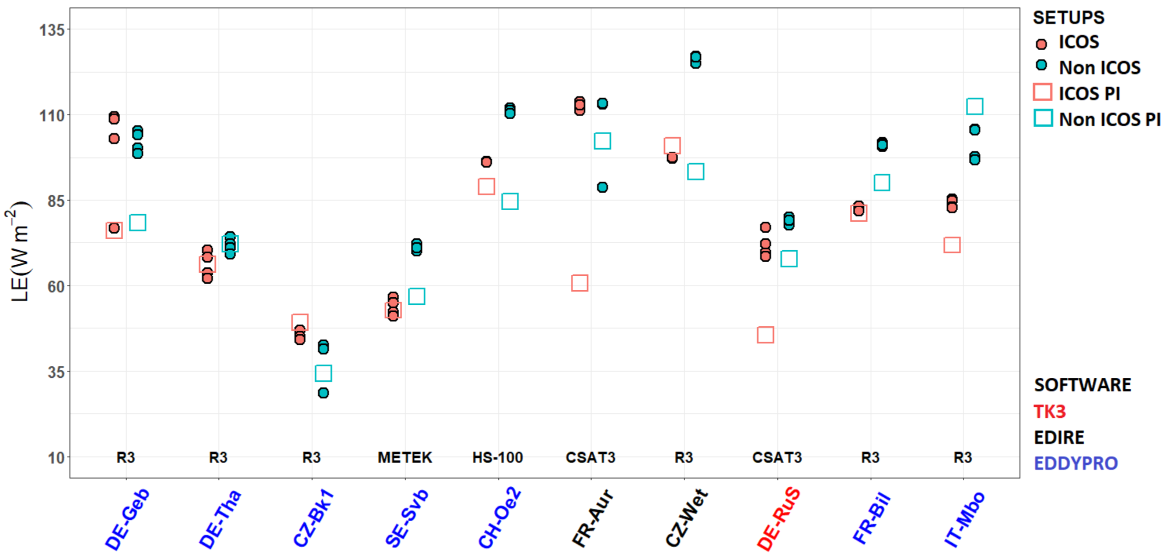

Figure 8 Averages of MDC of LE flux for three months of growing season. Red represents ICOS setup and cyan represents non ICOS setup. Circles represents fluxes calculated by ICOS processing square represents fluxes calculated by PIs. Four circles represent four processing schemes. Different colors of the labels of x-axis represent software used by PIs for flux calculations. Models of the sonic anemometers used in the non ICOS setups are mentioned at the base while for IRGA refer to figure 9.

Like for Fc, further evaluations are based on RMA regression model for the estimation of the effect of different setups and different processing on LE flux.

3.1.3.2 Effect of Different Setups on LE Flux

Effect of different setups on LE fluxes calculated using ICOS and PI processing strategies are displayed in **figure 9**. For LE flux the situation is heterogenous for both ICOS and PIs results. In ICOS processing, slopes between two setups with closed path IRGA are smaller than 1 at CZ-Bk1, resulting higher LE fluxes for ICOS setup, at DE-Geb and DE-Tha where the LE fluxes for ICOS setup are lower than non ICOS setup for ICOS processing strategies. PI processing is also consistent in terms of slope with ICOS for these sites.

For systems with open path IRGA type, ICOS processing slopes calculated between ICOS setup and non ICOS setups are in general higher than 1 except CH-Oe2 and FR-Aur. In PI processing 2 out of 6 sites produces higher LE fluxes obtained from ICOS setup. SE-Svb reported 31% (R^2 = 0.82) and 6% (R^2 = 0.98) lower LE flux from LI-7200 and HS-50 in comparison with LI-7200 and Metek, processed by ICOS and PI respectively.

For ICOS processing, on the whole differences observed between the fluxes calculated from ICOS and non ICOS setup are ranged between 1 % to 31 % with average variation of 11% and 1 % to 47 % for PI processing with average variation of 19 %. In ICOS processed fluxes R^2 ranges between 0.66 to 0.92 among different sites, whereas in PI processing R^2 ranges between 0.83 to 0.98. Like Fc, overall, ICOS processing scheme demonstrated higher mean absolute error between the LE fluxes from different setups as compared to PIs processing methods (except for FR-Aur, DE-RuS and IT-Mbo). Variability calculated by MAE varies between 17 – 41 W m^{-2} (27 W m^{-2} on average) for ICOS processing schemes of different setups and 6 – 40 W m^{-2} (21 W m^{-2} on average) for PIs processing.

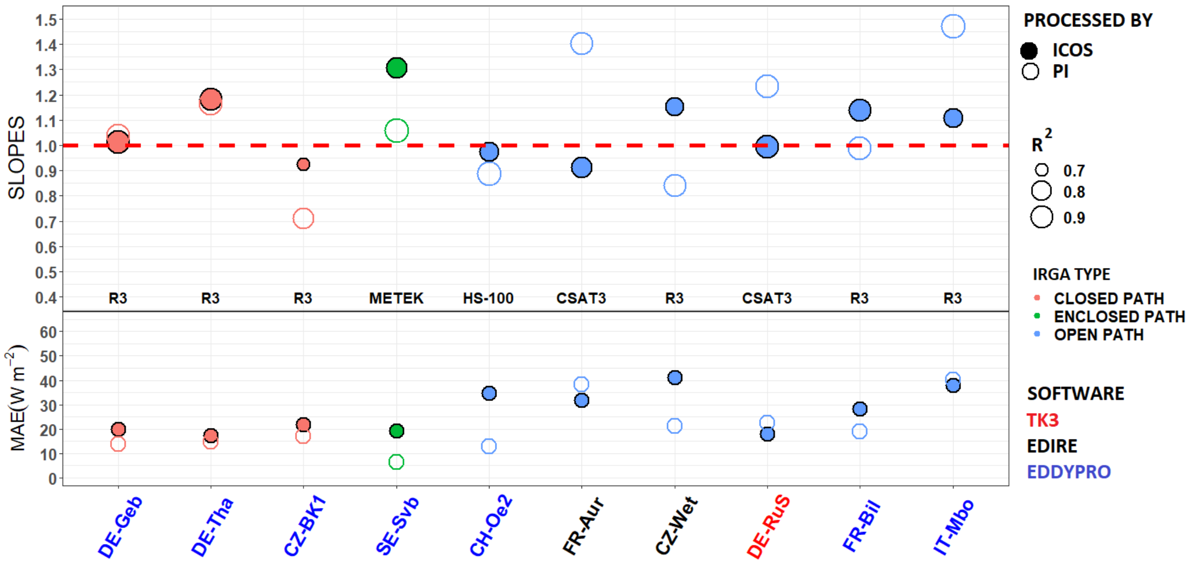

Figure 9 Effect of different setups on LE flux. Panel 1: Filled circles represent the slopes obtained from RMA regression between fluxes from two different (ICOS and non ICOS) setups using ICOS standard processing scheme, blank circles represent the slopes obtained from RMA regression between fluxes calculated by processing made by the site PI from ICOS and non ICOS setups. Size of the circle represents R^2. Red, green and blue colours represent closed, enclosed and open path IRGA for non ICOS setups. Red dashed line represents the 1:1 reference (slope=1). Different colors of the labels of x-axis represent software used by PIs for flux calculations. Models of the sonic anemometers used in the non ICOS setups are mentioned at the base. Panel 2: Filled circles represent the MAE between fluxes from ICOS and non ICOS setups processed using ICOS standard processing scheme and blank circles represent the MAE between fluxes calculated by processing made by the site PI from ICOS and non ICOS setups.

3.1.3.3 Effect of Different Processing on LE Flux

Figure 10 demonstrated that there are only three sites with closed path IRGA type. Results of ICOS and non ICOS setups are consistent at DE-Geb and DE-Tha, however at CZ-BK1 two processing methods are more comparable for ICOS setup in relation with non ICOS setup.

Slope for ICOS and non ICOS setups with open path IRGA are less than 1 explaining that LE fluxes from ICOS processing are higher than PI processing for both setups except for FR-Aur, IT-Mbo (non ICOS setup) and CZ-Wet (ICOS setup) where LE flux from PI processing is high. ICOS processing at SE-Svb reported 5 % (R^2 = 0.92) more LE flux for LI-7200 and HS-50 and 23 % (R^2 = 0.80) more LE flux for LI-7200 and Metek, as compared to PI processing. Altogether, For ICOS setup variation between two processing methods for LE flux ranged between 2 % to 34 % with 14 % difference on average (R^2 between 0.72 to 0.96). Whereas for non ICOS setup range is between 2 % to 25 % with 16 % difference on average (R^2 between 0.76 to 0.96) across different sites. MAE for LE flux is otherwise Fc, error between two processing for ICOS and non ICOS setups is 22 W m^{-2} on average. Range of error between ICOS and PIs processing methods varies from 8 to 53 W m^{-2} for ICOS setup and 11 to 36 W m^{-2} for non ICOS setup. Only FR-Aur is demonstration exceptional difference of error between two setups.

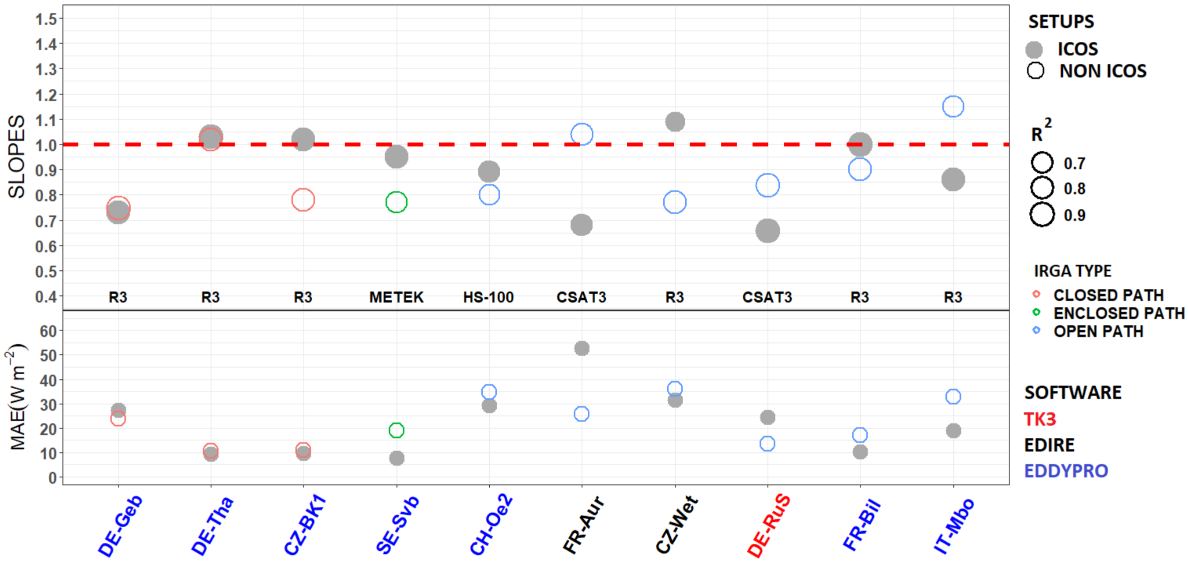

Figure 10 Effect of different processing schemes on LE flux including both calculation and filtering by Qc. Panel 1: Filled circles represent the slopes obtained from RMA regression between fluxes from ICOS and PIs processing schemes, using ICOS setup. Blank circles represent the slopes obtained from RMA regression between fluxes from ICOS and PIs processing schemes, using non ICOS setup. Size of the circle represents R^2. Red, green and blue colours represent closed, enclosed and open path IRGA non ICOS setups. Red dashed line is the 1:1 reference (slope=1). Different colors of the labels of x-axis represent software used by PIs for flux calculations. Models of the sonic anemometers used in the non ICOS setups are mentioned at the base. Panel 2: Filled circles represent the MAE between fluxes from ICOS and PI processing schemes using ICOS setup and blank circles represent the MAE between fluxes from non ICOS setup processed by PIs.

3.1.3.4 Differences in LE flux calculation (no filtering)

In comparison with the previous analysis (**figure 10**), slopes are closer to 1 in general because of the removal of filtering but in some cases, differences increased probably because of few data survived. Slopes of LE fluxes calculated from ICOS processing are less than 1 for both ICOS and non ICOS setup with closed path IRGA type except DE-Tha. For non ICOS setup with open path IRGA type slopes are less than 1 and ICOS processing is calculating high fluxes as compared to PI processing apart from IT-Mbo. For ICOS setup slopes are less than and ICOS processing calculating high LE flux from PI processing apart from CH-Oe2, CZ-Wet and FR-Bil. At SE-Svb ICOS processing of LE fluxes are 1 % higher for ICOS setup and 26 % higher for LI-7200 and Metek from PI processing. After the removal of filtering part, in general the MAE reduces by 5 W m^{-2} between two (ICOS and PIs) processing methods for ICOS and non ICOS setups but the range of variability of error increase and lies between 1 – 61 W m^{-2} for ICOS setup and 7 – 50 W m^{-2} for non ICOS setup. Exceptional increase in MAE is observed at FR-Aur (ICOS setup) and CZ-Wet (non ICOS setup)

Overall differences between ICOS processing and PI processing range between 1 % to 46 % for ICOS setup and 5 % to 28 % for non ICOS setup. On average the variation for ICOS and non ICOS setup is 14 % and 15 % among different sites. R^2 observed across different sites varies from 0.71 to 1 for ICOS setup and 0.84 to 1 for non ICOS setup processed differently (**figure 11**).

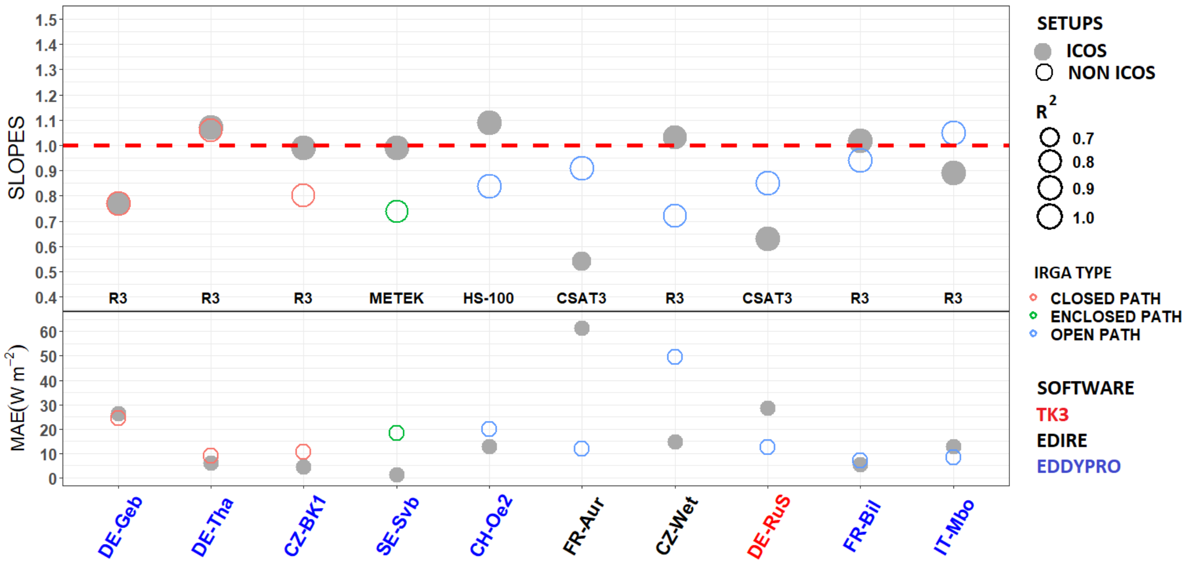

Figure 11 Effect of different processing schemes on LE flux (calculation only). Panel 1: Filled circles represent the slopes obtained from RMA regression between fluxes from ICOS and PIs processing schemes, using ICOS setup. Blank circles represent the slopes obtained from RMA regression between fluxes from ICOS and PIs processing schemes, using non ICOS setup. Size of the circle represents R^2. Red, green, and blue colours represent closed, enclosed and open path IRGA non ICOS setups. Red dashed line is the 1:1 reference (slope=1). Different colors of the labels of x-axis represent software used by PIs for flux calculations. Models of the sonic anemometers used in the non ICOS setups are mentioned at the base. Panel 2: Filled circles represent the MAE between fluxes from ICOS and PI processing schemes using ICOS setup and blank circles represent the MAE between fluxes from non ICOS setup processed by PIs.

3.1.3.5 LE Flux Filtered by ICOS and PIs Qc methods

Percentages of LE flux filtered by ICOS Qc method, PIs Qc methods and removed by both methods are presented in **figure 12**. LE flux filtered by ICOS Qc method ranges from 24 % to 95 % and by PIs QC methods 7 % to 45 % for ICOS setup across the sites. Commonly filtered bad quality flux by both ICOS and PI quality check tests range from 5 % to 42 %. In general percentage of data filtering by PIs Qc methods is less than ICOS, this is because of quality control tests of (Th. Foken & Wichura, 1996) that are common and included in all Qc methods applied by PIs as well as ICOS. In addition, with these tests ICOS applied set of other statistical tests (see **table 5**) for data filtering. Maximum percentage of LE filtration by both ICOS and PI is observed at FR-Pue where 42 % flux is removed during Qc filtering. For ICOS processing maximum data filtration is 95 % at FR-Lam and for PIs processing DE-RuS removed maximum bad quality data with percentage of 42. DE-RuS is the only case that filtered more data than ICOS.

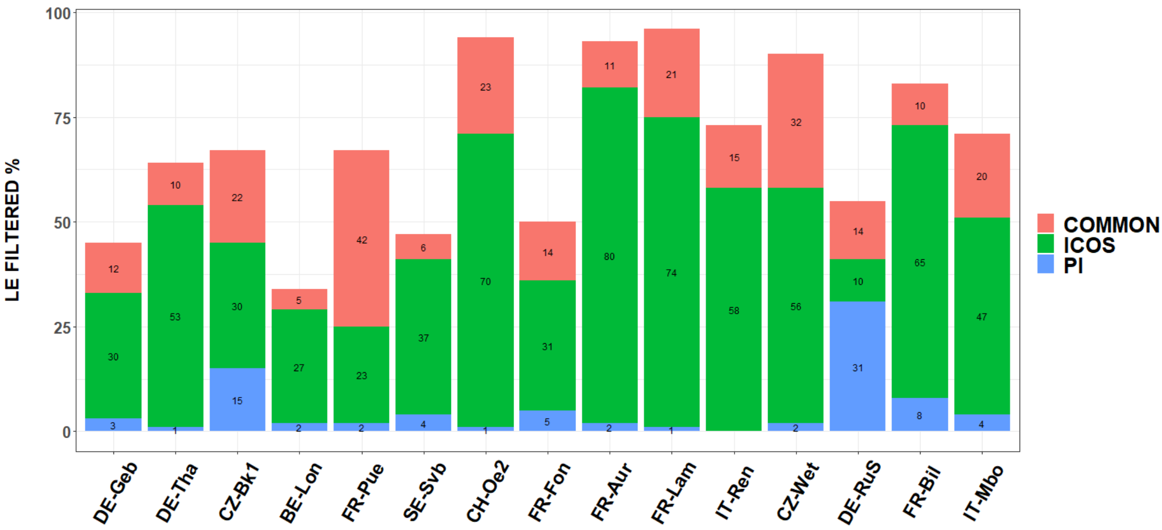

Figure 12 Percentage of LE flux filtered by PIs, ICOS and both simultaneously. Red colour represents percentage of LE flux filtered by both ICOS and PI, green colour represents percentage of LE flux filtered by ICOS only and blue colour represents LE flux filtered by PI only.

Like for Fc Further evaluation of filtering of LE flux in ICOS quality check tests (**figure 13)** determined that integral turbulence characteristics filtered minimum whereas EC system malfunction and disturbances filtered maximum percentage of LE flux across different sites for ICOS setup. Aberrant structural changes filtered 0 % to 19 %, EC system malfunction and disturbances filtered 7 % to 78 %, integral turbulence characteristics filtered 0 % to 1 %, low signal resolution filtered 0 % to 11 %, and non-stationary ratio by Mahrt (1998) filtered 0 % to 31 % LE flux.

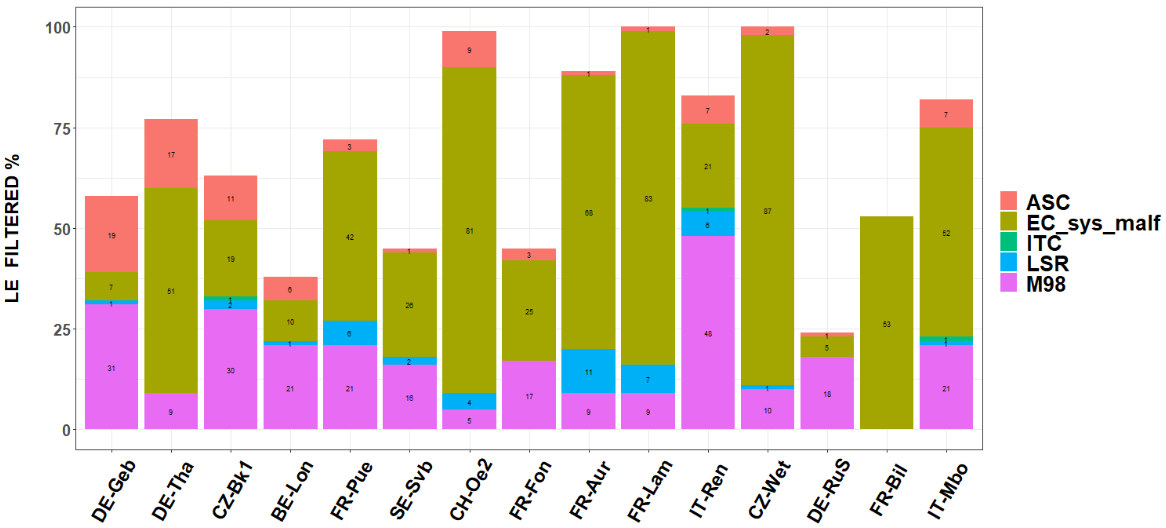

Figure 13 Percentage of data filtration for LE flux by quality control tests applied at ICOS. Different colours represent five different sources of error as classified in the original paper of Vitale at al., 2020.

3.1.4 Sensible Heat Flux (H)

Thirteen out of fifteen sites were used in the analysis of sensible heat flux. DE-Tha and IT-Mbo were not included because of data filtering more than 60 %.

3.1.4.1 Effect of 4 - Processing Schemes on H flux

There is a lot of consistency among the four processing for both ICOS and non ICOS anemometers **(figure 14).** This is because data obtained from only sonic anemometer is used for H flux calculation. However, analysis showed that, differences are still present in the fluxes from ICOS and PI processing. H fluxes from ICOS standardize anemometer, calculated from four processing schemes varies from 0.2 to 5.2 W m^{-2}, although H flux from non ICOS anemometer ranges from 0.1 to 14 W m^{-2}. Differences among four processing schemes for ICOS and non ICOS setups are 1.5 W m^{-2} and 2 W m^{-2} on average while, maximum range of variability is present only in one site (FR-Aur).

H fluxes obtained from HS-50 in parallel with R3, CSAT3 and Metek are also consistent. H fluxes processed by PI obtained from ICOS and non ICOS anemometers agreed with each other at CZ-Wet, other sites demonstrated the difference of 0.8 to 20 W m^{-2}. At CH-Oe2 and IT-Ren H fluxes were obtained only from HS-100 impaired with two different IRGAs, despite of same anemometer results showed minute difference in H flux. For ICOS anemometer average fluxes from PIs processing falls in the range of variability of ICOS setup at DE-Geb and CZ-Bk1. On other sites average fluxes variers from 0.3 to 22 W m^{-2}. For non ICOS anemometers, fluxes from PIs processing fall in the range of ICOS processed results at DE-Geb and FR-Lam. Differences ranged between 0.6 to 22 W m^{-2}.

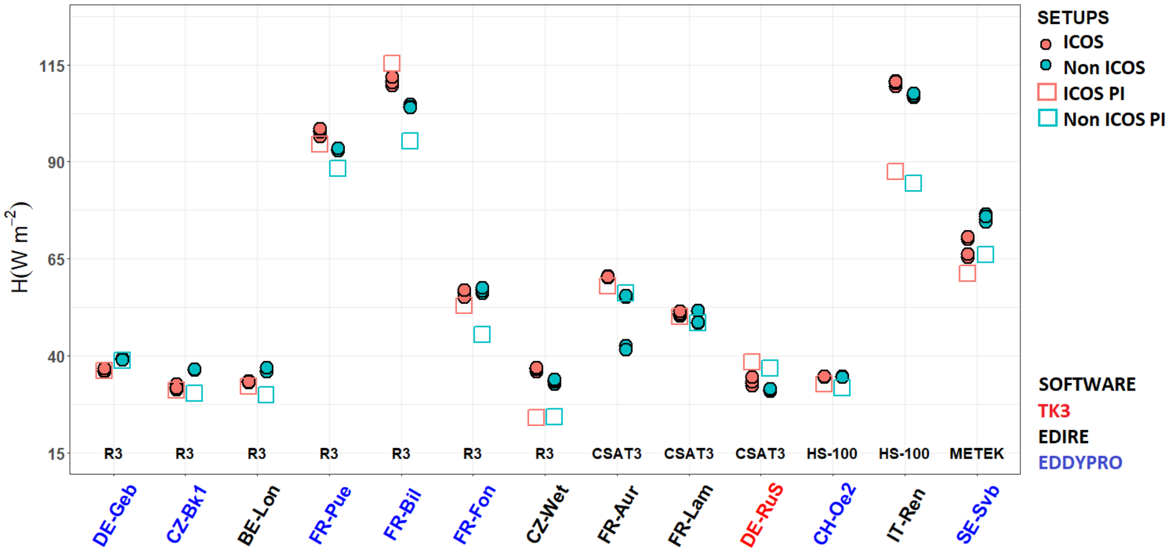

Figure 14 Averages of MDC of H flux for three months of growing season. Red represents ICOS setup and cyan represents non ICOS setup. Circles represent fluxes calculated by ICOS processing, square represents fluxes calculated by PIs. Four circles represent four processing schemes. Different colors of the labels of x-axis represent software used by PIs for flux calculations.

3.1.4.2 Effect of Different Anemometers on H Flux

Differences observed between the H fluxes obtained from two different anemometers are ranged between 1 % to 19 % with R^2 varied between 0.90 to 0.99 for ICOS and 1 % to13 % with R^2 ranged between 0.89 to 0.99 for PI processing across different sites. Overall variation between ICOS and non ICOS setup is 7 % and 5 % on average for ICOS and PI processing Slopes for two different anemometers are close to 1 for ICOS (except CZ-BK1 and BE-Lon) and PI processed fluxes (**figure 15**).

H fluxes from ICOS anemometers are smaller than R3 at DE-Geb, CZ-Bk1 and BE-Lon and higher at FR-Pue, FR-Bil and FR-Fon whereas at CZ-Wet there is no difference observed between the H fluxes obtained from two different anemometers (ICOS processing). Oppositely H fluxes processed by PIs obtained from ICOS anemometer is higher than R3 except at DE-Geb and BE-Lon. H fluxes obtained from HS-50 are higher as compared to CSAT3 except at FR-Lam (slope = 1 in PI results)

At CH-Oe2 and IT-Ren, HS-100 is used with two different types of IRGA but sill demonstrating small variation in the fluxes both in ICOS and PIs results at CH-Oe2. PI processing showed more variation (11 %) as compared to ICOS (3 %) between flux from HS-50 and Metek. Comparably Fc and LE flux, mean absolute error between H flux obtained from two anemometers is slightly higher in ICOS processing in relation to non ICOS processing. It is 13 and 10 W m^{-2} on average for ICOS and PIs processing methods. Among all the sites MAE between ICOS processed H flux obtained from different anemometers (6 – 22 W m^{-2}) is not much diverse from PIs processed H flux (1 – 26 W m^{-2}).

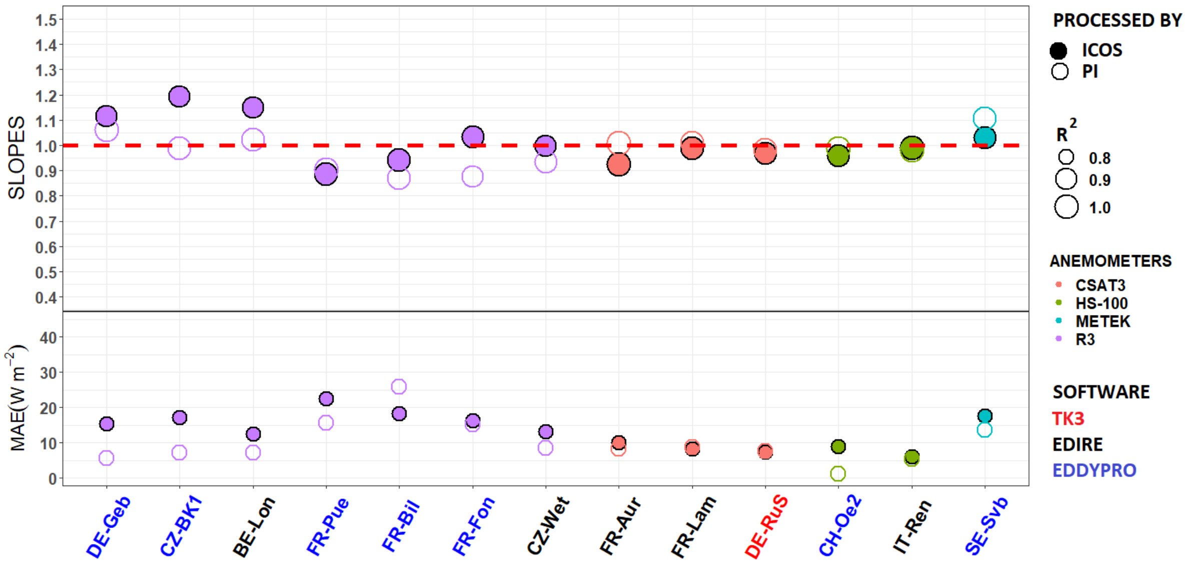

Figure 15 Effect of different setups on H flux. Panel 1: Filled circles represent the slopes obtained from RMA regression between fluxes from two different (ICOS and non ICOS) anemometers using ICOS standard processing scheme, blank circles represent the slopes obtained from RMA regression between fluxes calculated by processing made by the site PI from ICOS and non ICOS anemometers. Size of the circle represents R^2. Different colours represent models different of sonic anemometers. Red dashed line represents the 1:1 reference (slope=1). Different colors of the labels of x-axis represent software used by PIs for flux calculations. Panel 2: Filled circles represent the MAE between fluxes from ICOS and non ICOS setups processed using ICOS standard processing scheme and blank circles represent the MAE between fluxes calculated by processing made by the site PI from ICOS and non ICOS anemometers.

3.1.4.3 Effect of Different Processing on H Flux

Regression analysis in **figure 16** pointed in higher H fluxes obtained from HS-50 processed by using ICOS strategy as compared to PI processing except at CZ-BK1 and DE-RuS. HS-50 is resulting less differences as slopes are closer to unity as compared to R3 except at FR-Pue, where both anemometers calculated almost consistent fluxes. Fluxes from two processing for CSAT3 are more comparable in relation with HS-50. At CH-Oe2 and IT-Ren H fluxes from same sonic anemometer differed 11 % to 20 % and 9 % to 20 % when processed by using ICOS and PIs strategies at respective sites. At SE-Svb, H fluxes calculated from ICOS processing are 12 % and 6 % higher than PI processing for HS-50 and Metek. IT-Ren has maximum MAE between the H flux processed differently for both ICOS and non ICOS anemometers. Overall variability of error between different processing methods is comparable for two anemometer types (ICOS and non ICOS) among sites. There is an average error of 14 W m^{-2} in H flux processed by ICOS and PIs methods for both anemometer types. MAE varies from 9 – 39 W m^{-2} for ICOS and 6 – 41 W m^{-2} for non ICOS anemometer.

Mainly, and to conclude, differences calculated between ICOS and PI processing strategies ranged between 1 % to 23 % with average difference of 10 % for ICOS anemometer and 2 % to 28 % with average difference of 12 % for non ICOS anemometers. Minimum R^2 observed is 0.79 and 0.77, maximum is 0.98 and 0.99 for ICOS standard sonic anemometer and non ICOS sonic anemometers across sites.

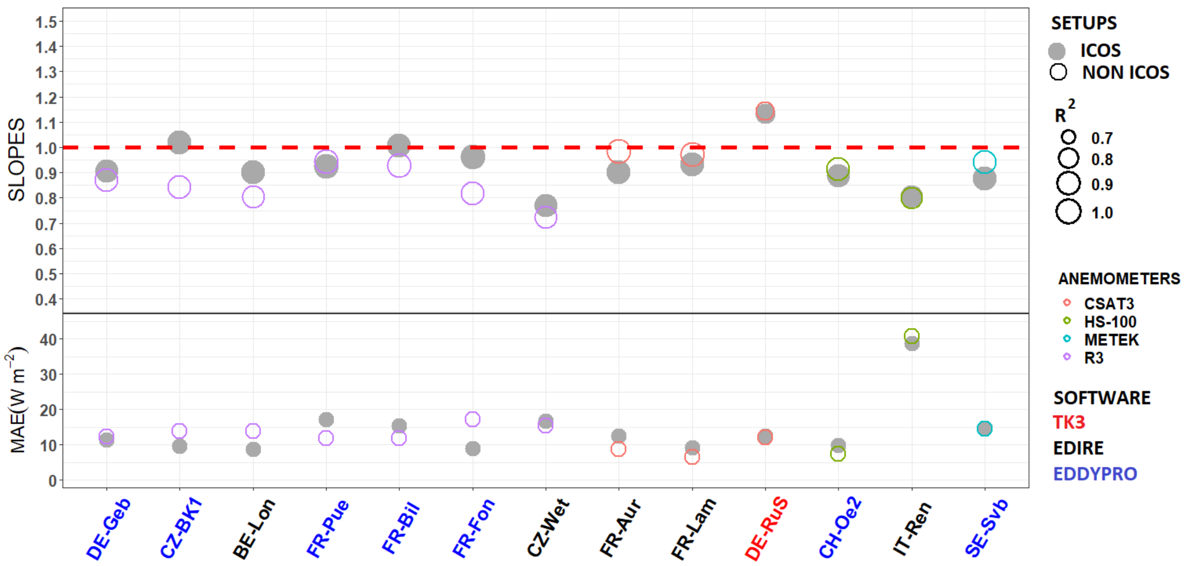

Figure 16 Effect of different processing schemes on H flux including both calculation and filtering by Qc. Panel 1: Filled circles represent the slopes obtained from RMA regression between fluxes from ICOS and PIs processing schemes, using ICOS anemometer. Blank circles represent the slopes obtained from RMA regression between fluxes from ICOS and PIs processing schemes, using non ICOS anemometer. Size of the circle represents R^2. Different colours represent models of different sonic anemometers. Red dashed line is the 1:1 reference (slope=1). Different colors of the labels of x-axis represent software used by PIs for flux calculations. Panel 2: Filled circles represent the MAE between fluxes from ICOS and PI processing schemes using ICOS setup and blank circles represent the MAE between fluxes from non ICOS setup processed by PIs.

3.1.4.4 Differences in H flux calculation (no filtering)

Comparison of two processing schemes focusing calculation only reduced the difference between two processing. Average variation observed between ICOS and PI processing is 3 % and 5 % for ICOS and non ICOS setups. For ICOS anemometer they ranged between 1 % to 14 % and 2 % to 15 % for non ICOS anemometers with R^2 ranges between 0.99 to 1 for both ICOS and non ICOS sonic anemometers (**figure 17**). As mentioned above ICOS processing is calculating higher fluxes for both ICOS and non ICOS anemometer in maximum number of sites probably because of filtering of number of small fluxes (near zero), however this is not valid in analysis of calculation only. Mean absolute error also reduces significantly for H flux to 4 and 6 W m^{-2} for ICOS and non ICOS anemometers with the range of 1 – 19 W m^{-2} and 0.2 – 19 W m^{-2}. After removal of filtering, H flux obtained from different anemometers enumerated almost same MAE between ICOS and non ICOS processing at FR-Pue, FR-Aur, DE-RuS, CH-Oe2 and IT- Ren.

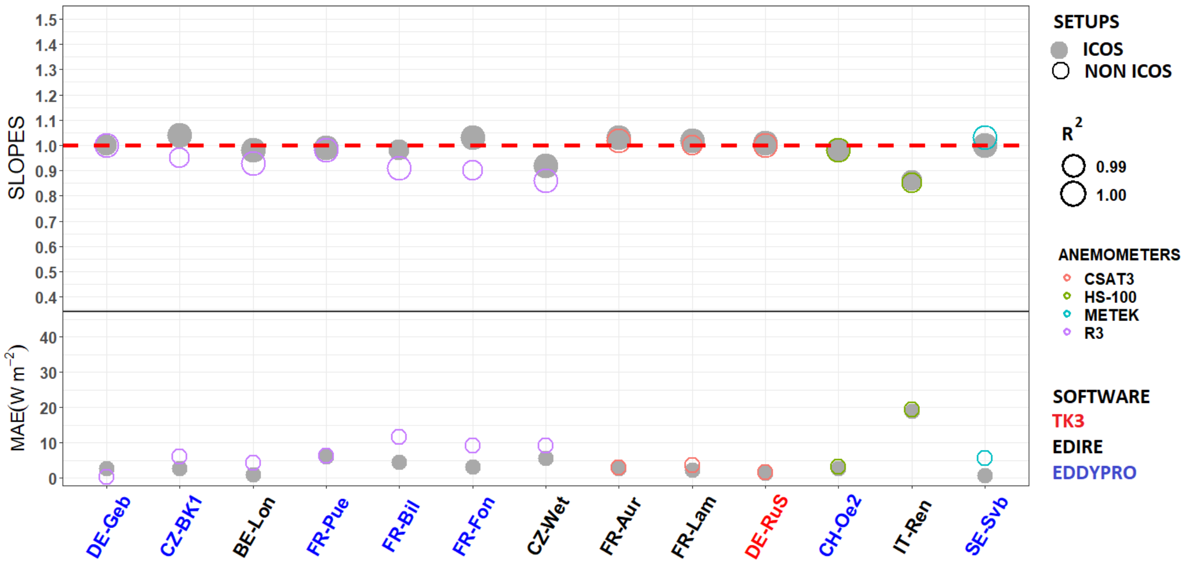

Figure 17 Effect of different processing schemes on H flux (calculation only). Panel 1: Filled circles represent the slopes obtained from RMA regression between fluxes from ICOS and PIs processing schemes, using ICOS anemometer. Blank circles represent the slopes obtained from RMA regression between fluxes from ICOS and PIs processing schemes, using non ICOS anemometer. Size of the circle represents R^2. Different colours represent models of different sonic anemometers. Red dashed line is the 1:1 reference (slope=1). Different colors of the labels of x-axis represent software used by PIs for flux calculations. Panel 2: Filled circles represent the MAE between fluxes from ICOS and PI processing schemes using ICOS setup and blank circles represent the MAE between fluxes from non ICOS setup processed by PIs.

3.1.4.5 H Flux Filtered by ICOS and PIs Qc Methods

ICOS procedure is only one that applied filtering on H flux. ICOS quality check methods filtered 21 % to 99 %, while 7 % to 46 % H flux is filtered in PIs. 4 % to 23 % filtering is common in both (**figure 18**). Maximum percentage of H flux filtration by both ICOS and PI is observed at IT-Ren where 23 % flux is removed during Qc filtering. For ICOS processing maximum data filtration is 99 % that is only at DE-Tha due to aberrant structural changes (change in variance and abrupt shift in mean) and for PIs processing maximum removal of bad quality data is 44 % at DE-RuS, only site that filters more than ICOS in all three fluxes.

In the analysis of data filtering by systematic errors for H flux, integral turbulence characteristics filtered minimum whereas non-stationary ratio by Mahrt (1998) filtered maximum percentage of H flux in general. Aberrant structural changes filtered 0 % to 74 %, EC system malfunction and disturbances filtered 4 % to 24 %, integral turbulence characteristics filtered 0 % to 1 %, low signal resolution filtered 0 % to 15 %, and non-stationary ratio by Mahrt (1998) filtered 0 % to 33 % H flux (**figure 19**).

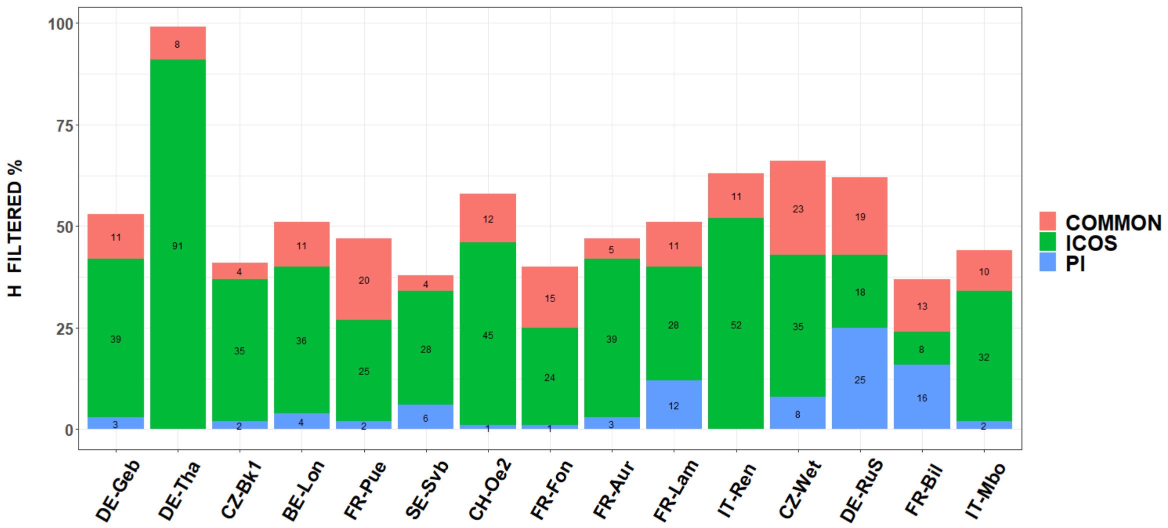

Figure 18 Percentage of H flux filtered by PIs, ICOS and both simultaneously. Red colour represents percentage of H filtered by both ICOS and PI, green colour represents percentage of H flux filtered by ICOS only and blue colour represents H flux filtered by PI only.

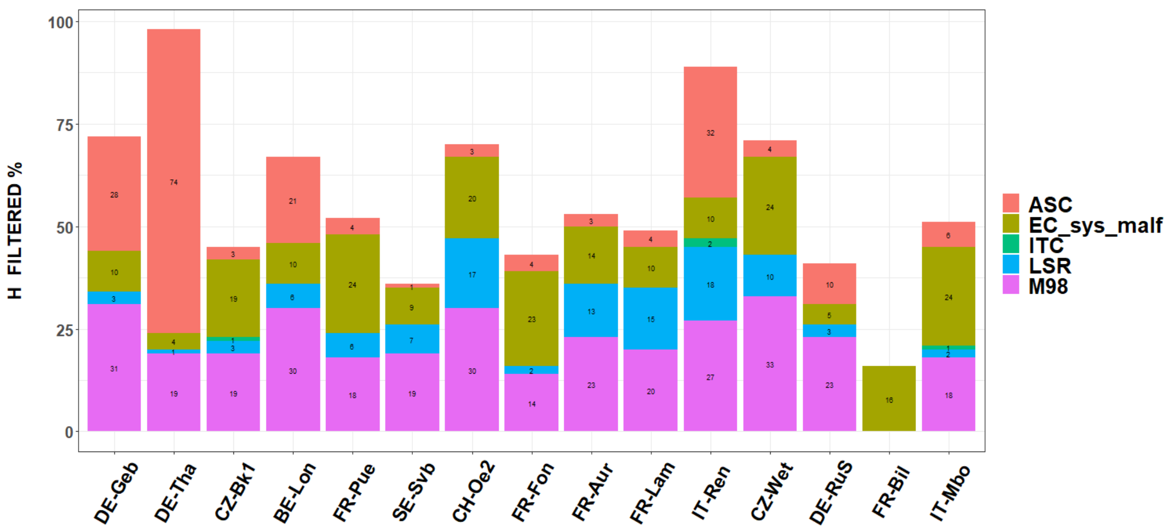

Figure 19 Percentage of data filtration for H flux by quality control tests applied at ICOS. Different colours represent five different sources of error as classified in the original paper of Vitale at al., 2020.

3.2 Overall Effect of Different setups and Processing schemes on Fluxes

Results of RMA regression model (slope and R^2) and MAE already presented in figure 3, 4 & 5) are summarized in **figure 20**. Mark inside the box represent median of the range, edges are upper and lower quartiles, dots represent outliers. Blue dashed line is reference line indicating slope 1. Value of slope less than 1 indicates that ICOS setup or ICOS processing scheme calculating higher fluxes than non ICOS setup or processing. The explanation of analysis is based on the median of all the slopes and R^2 calculated for different setups and processing schemes for selected sites. Results confirmed that the median of the R^2 for Fc calculated between ICOS and non ICOS setup and processed by ICOS is 0.93 (slope - 0.06) and while it is 0.96 (slope 0.03) when processed by PIs. Mean absolute error between two setups processsed by ICOS and PIs 1.7 and 1.3 µmol $CO_2m^{-2}\ s^{-1}$.

In the comparison between two different processing of same setup, Fc processed by ICOS and PIs has 0.98 R^2 for ICOS and 0.95 for non ICOS setup. Slopes from two different processings for both setups are less than 1, revealing that fluxes processed by ICOS methods are on average 6 % larger than PIs processing for ICOS setup with 1 µmol $CO_2m^{-2}\ s^{-1}$ MAE and 13 % larger for non ICOS setup with µmol 1.6 $CO_2m^{-2}\ s^{-1}$MAE. Regression analysis only on the calculations considering commom half hours reduces the variabilty between Fc processed by ICOS and PIs for both setups up to 3 % for ICOS setup and 13 % for non ICOS setup. The value of R^2 also improves for both setups, Fc from ICOS setup and non ICOS setup processed by ICOS and PIs has 1 and 0.98 R^2. MAE calculted between ICOS and PIs processing setup while considering only calculations is 0.6 and 1.1 µmol $CO_2m^{-2}\ s^{-1}$ for ICOS and non ICOS setups.

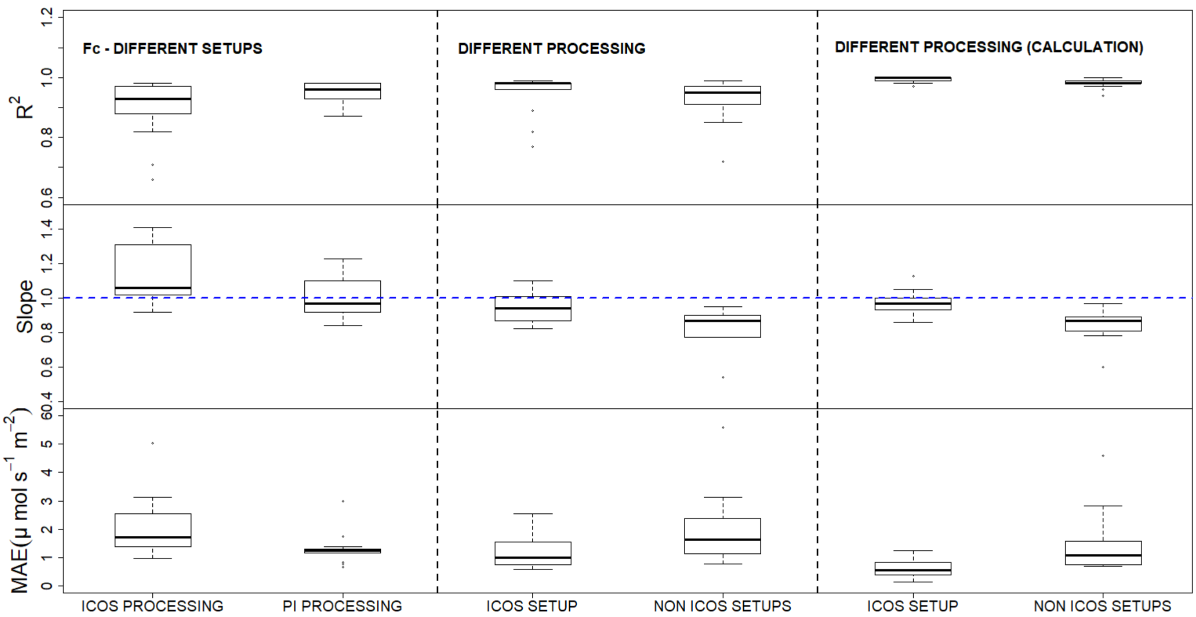

Figure 20 Box plots indicates range of R^2, slope and MAE for Fc. R^2 and slope obtained from RMA regression analysis of fluxes between (left to right) panel 1: ICOS and non ICOS setup processed by ICOS strategies and PIs, panel 2: ICOS and PIs processing for ICOS and non ICOS setups including both calculation and filtering and panel 3: ICOS and PIs processing for ICOS and non ICOS setups including only calculations. The mark inside the box indicates the median, the edges are upper and lower quartiles. Dots represents the outliers. Blue dashed line is the 1:1 reference (slope=1).

There is high level of variability in Fc among sites due to different setups although the median is close to 1. ICOS processing is also playing a role with in general larger fluxes and variability present in different processing strategies is mostly due to filtering as it significantly reduced when only calculations were compared. Large variability between two setups processed by ICOS methods is due to CZ-Wet (shows maximum slope and MAE).

There is large variability in fluxes processed by PIs in relation with ICOS processing between two setups even though the median is close to 1. Slope for ICOS processed LE is -0.06 (R^2 0.82) and for PI processing, it is -0.05 (R^2 0.92) whereas, MAE present in ICOS and PIs processing methods are 25 W m^{-2} and 18 W m^{-2} respectively. ICOS processing strategy is producing 8 % (MAE = 22) and 18 % (MAE = 21) larger fluxes with 0.93 and 0.90 R^2 for ICOS non ICOS setups. Variablity between two processing is larger as compared to Fc. Analysis without filtering pointed out that variability is still present in two processing methods, while the differences between two processing reduced up to 1% and 16% for both setups with 0.98 R^2 and 13 W m^{-2} and W m^{-2} MAE . LE is more complex flux, or it may be less investigated, with fewer standardized and optimized techniques (**figure 21**).

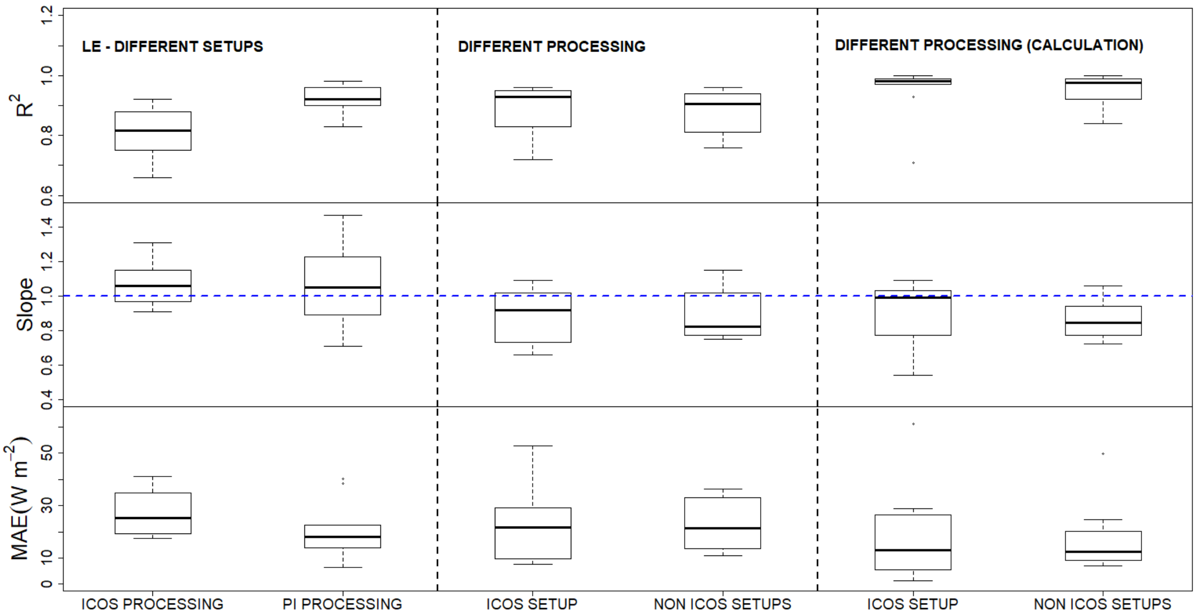

Figure 21 Box plots indicates range of R^2, slope and MAE for LE flux. R^2 and slope obtained from RMA regression analysis of fluxes between (left to right) panel 1: ICOS and non ICOS setup processed by ICOS strategies and PIs, panel 2: ICOS and PIs processing for ICOS and non ICOS setups including both calculation and filtering and panel 3: ICOS and PIs processing for ICOS and non ICOS setups including only calculations. The mark inside the box indicates the median, the edges are upper and lower quartiles. Dots represents the outliers. Blue dashed line is the 1:1 reference (slope=1).

In H flux median is close to 1 but small variability is present between two anemometers as compared to Fc and LE flux, probably because of one sensor (**figure 22**). Median of slope are 0.01 with R^2 0.92 and 0.97 for ICOS and PI processed H flux. MAE for ICOS and PIs processed fluxes are 13 W m^{-2} and 18 W m^{-2}. Likewise, Fc and LE, ICOS processing is calculating higher H flux in relation with PIs processing by 9 % with 12 W m^{-2} MAE (0.94 and 0.95 R^2) for both ICOS and non ICOS anemometer. Variability Present between two processing schemes are due to filtering as it removes small fluxes and reduced the differences between two processing methods for ICOS anemometer (slope =1) and non ICOS anemomete (slope = 0.02) with R^2 =1. Removal of filtering also reduced MAE to 3 W m^{-2} and 6 W m^{-2}.

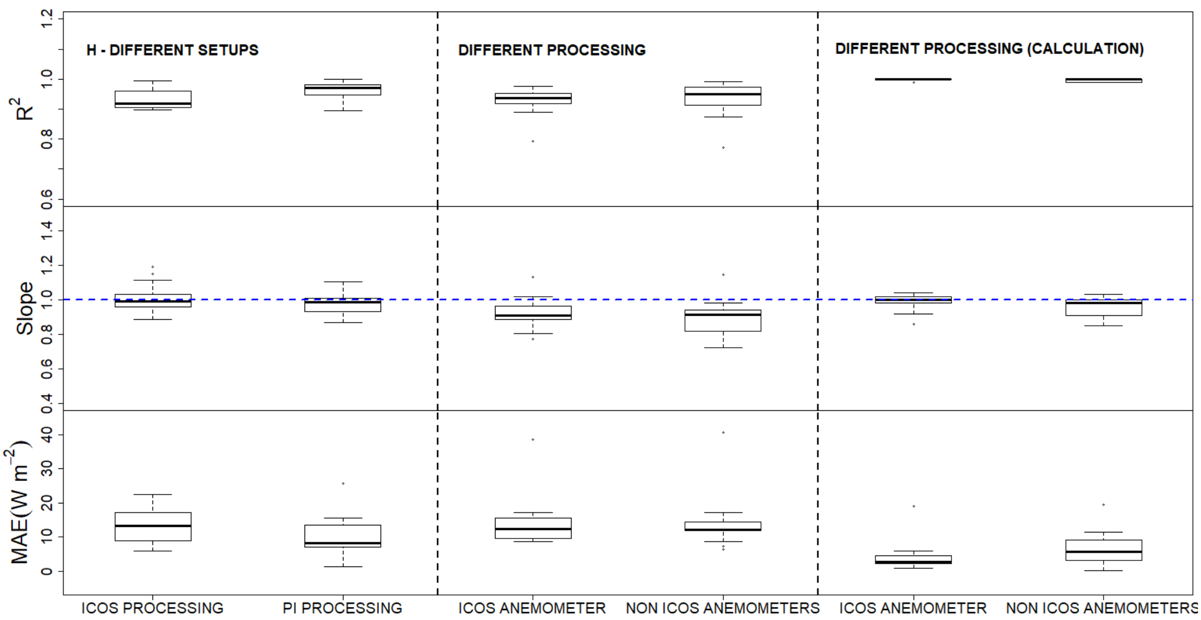

Figure 22 Box plots indicates range of R^2, slope and MAE for H flux. R^2 and slope obtained from RMA regression analysis of fluxes between (left to right) panel 1: ICOS and non ICOS anemometers processed by ICOS strategies and PIs, panel 2: ICOS and PIs processing for ICOS and non ICOS anemometers including both calculation and filtering and panel 3: ICOS and PIs processing for ICOS and non ICOS anemometers including only calculations. The mark inside the box indicates the median, the edges are upper and lower quartiles. Dots represents the outliers. Blue dashed line is the 1:1 reference (slope=1).

3.3 Reprocessing of Long-term Data

In the second part of the activity raw data for long timeseries (between 6 to 20 years) were reprocessed using the 4 processing option combinations for rotation and detrending methods for 9 ICOS sites. PIs of ICOS sites had changed their existing setups and shifted to the new setup few years back. This long-term dataset of 9 sites has data from at least two different setups in long timeseries. Part of the dataset before shift of setup is referred as non ICOS and after the shift of setup is referred as ICOS dataset. For comparison, results from only one processing option are used. The selection of the processing combination was driven by similarity to the selection of the PIs in their own processing. For all the sites this corresponds to DR and BA for coordinate rotation and signal detrending respectively, except CZ-Bk1 and DE-Tha which selected PF for coordinate rotation. Study explains difference between the two processing up to the year with non ICOS setup, interannual variability within PIs processing and ICOS processing and effect of shift of setup on fluxes in the sites with more than one year of ICOS setup. BE-Lon and DE-Geb are crop lands, difference in the calculated fluxes among years are also generated from different crops cultivated in the years due to rotation.

3.3.1 CO_2 Flux (Fc)

Averages of Fc calculated from MDC of six subsets made from three months of growing season of each year for all the sites are exhibited in **figure 23.** For croplands three months were selected from growing season of crop. In the figure are also reported the years with the ICOS setup that ranges between 1 and 7, clearly always at the end of the timeseries. In 7 out of 9 sites closed path IRGA was used before shifting to LI-7200 and R3 has been working on 7 sites before shifting to HS-50. In the FI-Hyy and FI-Sii sites R2 and Metek sonics, while at CZ-Wet and FR-Bil open path IRGAs were used. Analysis revealed that Flux calculated by ICOS processing are in general lower as compared to PI processing in most of the years across different sites. The difference is quite variable across sites and the maximum agreement is present in FR-Pue. Differences in Fc fluxes processed by ICOS and PIs of sites vary between 0.6-2.2 µmol CO_2m^{-2} s^{-1} at BE-Lon, 0.5-0.9 µmol CO_2m^{-2} s^{-1} at CZ-Bk1, 0.07-1.5 µmol CO_2m^{-2} s^{-1} at CZ-Wet, 0.1-5.7 µmol CO_2m^{-2} s^{-1} at DE-Geb 0.2-1.6 µmol CO_2m^{-2} s^{-1} at DE-Tha, 0.08-0.3 µmol CO_2m^{-2} s^{-1} at FI-Hyy, 0.5-0.9 µmol CO_2m^{-2} s^{-1} at FI-Sii, 0.07-0.16 µmol CO_2m^{-2} s^{-1} at FR-Bil and 0.01-0.5 µmol CO_2m^{-2} s^{-1} at FR-Pue. Minimum variation witnessed between two processing among all the sites is 0.01 µmol CO_2m^{-2} s^{-1} at FR-Pue (2003) and maximum is 5.7 µmol CO_2m^{-2} s^{-1} at DE-Geb (2005). Despite the differences in each site the trend in the interannual variability is similar for both ICOS and PI processing schemes.

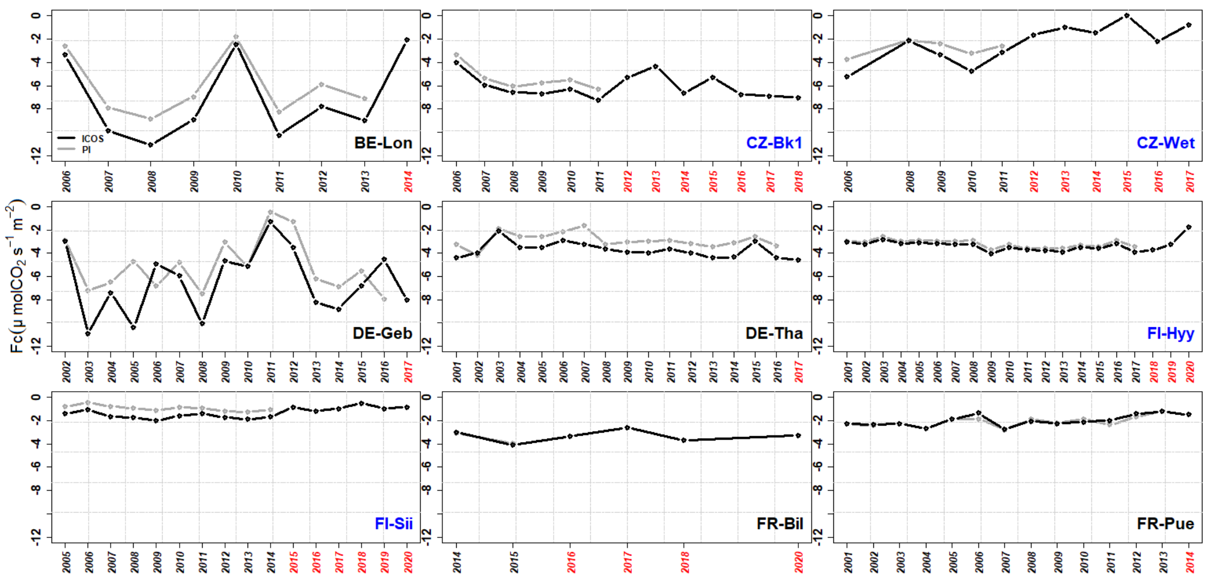

Figure 23 Averages of MDC of Fc calculated from three months of growing season of each year. Black and grey lines represent ICOS and PI processing. Years in red are representing shift to the ICOS setup. Sites with blue colour have more than one year with ICOS setup.

3.3.2 Latent Heat Flux (LE)

Similar analysis that has been done for the Fc, also for LE the flux have been compared in **figure 24**. In this case however ICOS processing calculated higher fluxes as compared to PI processing in most of the years across different sites. There is exception at DE-Tha (2008), FI-Sii (2009) and FR-Pue (2001, 2002, 2004, 2006 and 2011) where, LE fluxes calculated by ICOS processing were smaller than PI processing, but differences are in general small or, like in the case of FR-Pue in series with a lot of interannual variability. Also, for LE flux even though with the variations in each site, the trend in the interannual variability is similar for both ICOS and PI processing except for FR-Pue where there is no agreement in the year-to-year variability. Differences in averages of LE fluxes processed by ICOS and PIs of sites range between 28-55 W m^{-2} at BE-Lon, 19-40 W m^{-2} at CZ-Bk1, 33-52 W m^{-2} at CZ-Wet, 21-63 W m^{-2} at DE-Geb, 1-13 W m^{-2} at DE-Tha, 5-17 W m^{-2} at FI-Hyy, 1-16 W m^{-2} at FI-Sii, and 4-54 W m^{-2} at FR-Pue. For LE flux only one year with non ICOS setup is available at FR-Bil the difference observed between two processing is 1.5 W m^{-2}. Minimum and maximum change noted in the LE flux processed by ICOS and PIs among all the sites are 1 $W^{-1}m^{-2}$ at DE-Tha (2006) and FI-Sii (2014) and 63 W m^{-2} at DE-Geb (2003).

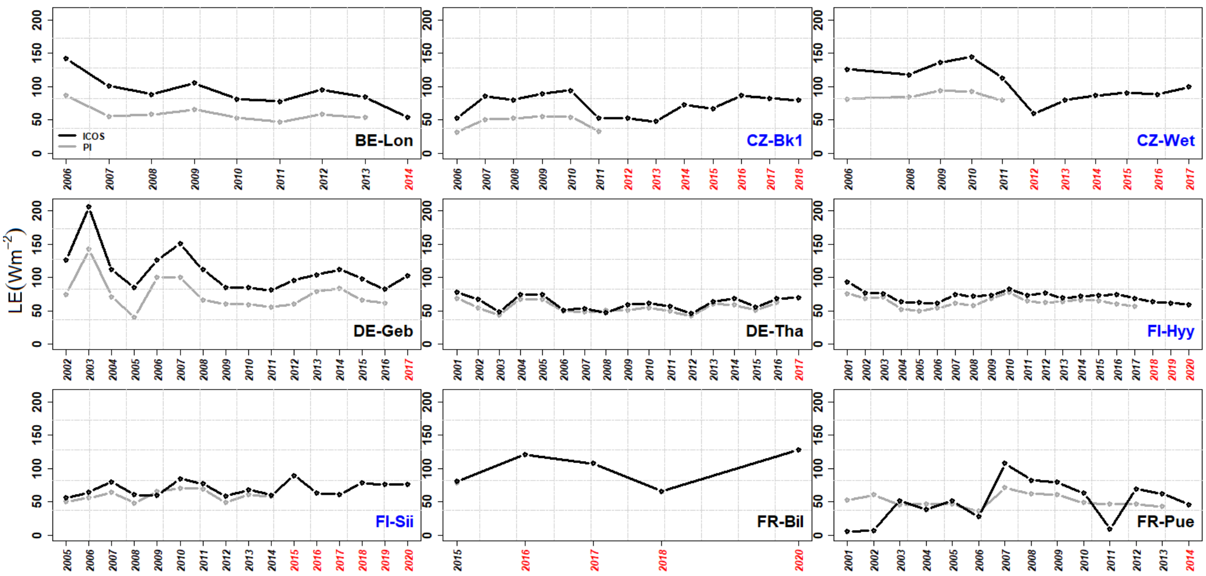

Figure 24 Averages of MDC of LE flux calculated from three months of growing season of each year. Black and grey lines represent ICOS and PI processing. Years in red are representing shift to the ICOS setup. Sites with blue colour have more than one year with ICOS setup.

3.3.3 Sensible Heat Flux (H)

Likewise in LE flux, higher fluxes have been calculated by ICOS processing with respect to PI processing in most of the years across different sites. Like LE flux there is also exception where

ICOS processing is also lower than PI processing in few years from the long time series available at DE-Geb, DE-Tha and FR-Bil. Even though there is variation in calculated fluxes among years in each site, the trend in the interannual variability is similar for both ICOS and PI processing except for DE-Geb (2002 and 2003). Best agreement is found in BE-Lon. Minor differences are observed over all that ranged between 0.1-9 W m^{-2} at BE-Lon, 11-18 W m^{-2} at CZ-Bk1, 1-11 W m^{-2} at CZ-Wet, 0.2-19 W m^{-2} at DE-Geb, 6-20 W m^{-2} at DE-Tha, 6-22 W m^{-2} at FI-Hyy, 1-7 W m^{-2} at FI-Sii, 2-6 W m^{-2} at FR-Bil and 6-14 W m^{-2} at FR-Pue. Minimum and maximum difference noticed in the H flux processed by ICOS and PIs among all the sites are 0.1 W m^{-2} at BE-Lon (2012) and 22 W m^{-2} at FI-Hyy (2017) (**figure 25**).

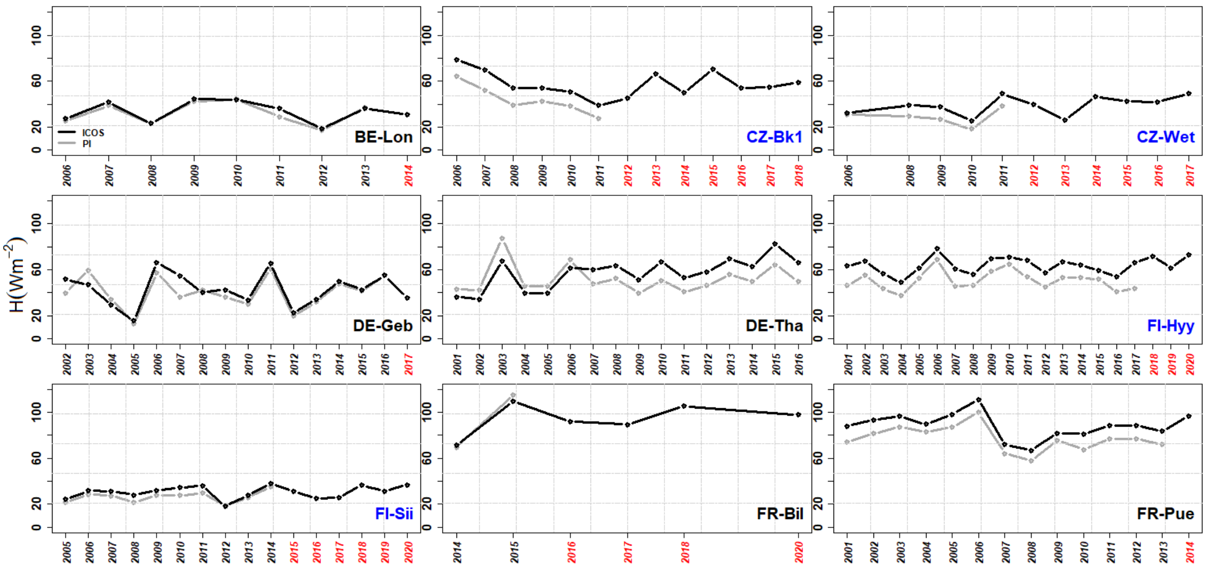

Figure 25 Averages of MDC of H flux calculated from three months of growing season of each year. Black and grey lines represent ICOS and PI processing. Years in red are representing shift to the ICOS anemometer. Sites with blue colour have more than one year with ICOS anemometer.

3.4 Regression analysis of Long-term Data

For long-term data further analysis has been done by selecting sites having raw EC data from ICOS setup for more than two years. MDC of six subsets from 3 months of growing season of each year for all the sites were used in this analysis for all three fluxes. Each year (6*48 values) is regressed against all the other years (with the same setup and with the different setup) and for both the ICOS and the PI processing. Processed Fc from CZ-Bk1, CZ-Wet, FI-Hyy and FI-Sii have been used to investigate the effect of reprocessing on fluxes and interannual variability because there are enough years with both the ICOS and non-ICOS setup periods.

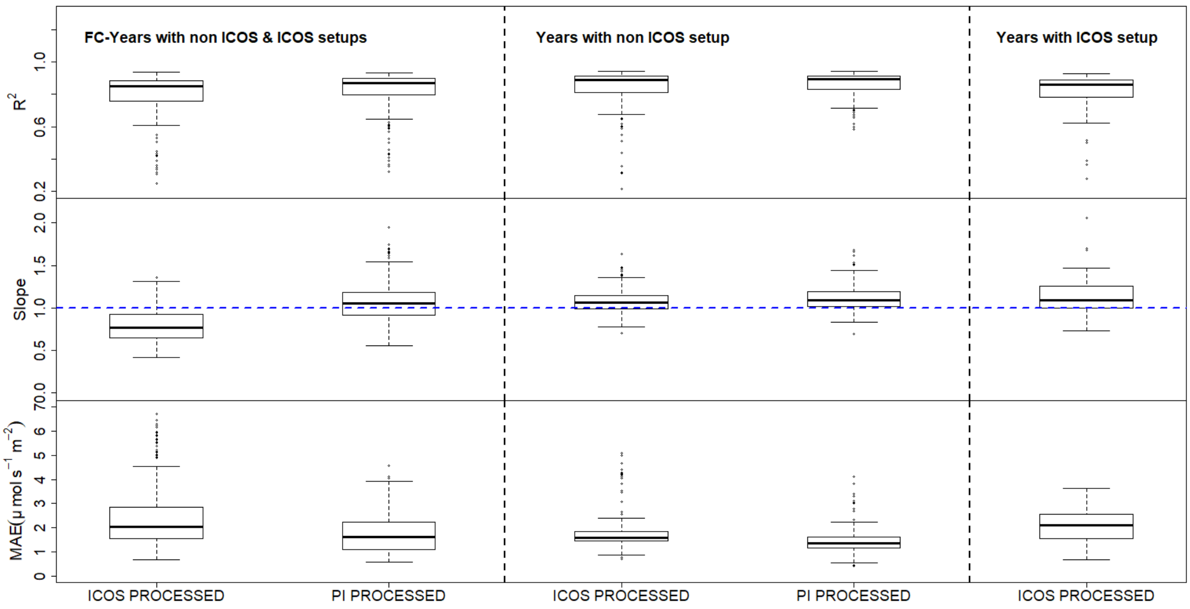

Figure 26 Box plots indicates range of R^2, slope and MAE for Fc. R^2 and slope obtained from RMA regression analysis of fluxes between (left to right) panel 1: all the years of non ICOS setup vs ICOS setup processed by ICOS and PIs, panel 2: all the years of non ICOS setup processed by ICOS and PIs and panel 3: all the years of ICOS setup. The mark inside the box indicates the median, the edges are upper and lower quartiles. Dots represents the outliers. Blue dashed line is the 1:1 reference (slope=1).

Figure 26 summarizes the results of this analysis for Fc. In Panel 1 (left to right) R^2 and slopes are calculated by applying RMA regression among Fc obtained from all the years of non ICOS setup against all the years with ICOS setup (in the regression non ICOS on the x axis) both processed by ICOS (left boxplot) and PIs (right boxplot). This plot shows the general consistency of the fluxes in the two periods that is influenced by both the natural interannual variability plus disturbances and the change of system to the ICOS setup. In panel 2 the same is done however only among all the years from non ICOS setup processed by ICOS and PIs to check the interannual variability with the same EC system (non ICOS) and in panel 3 the same was done only using all the years of ICOS setup processed by ICOS. Mean absolute error was also calculated for above mentioned datasets. Mark inside the box represent median of the range, edges are upper and lower quartiles, dots represent outliers. Blue dashed line is reference line indicating slope 1.

Variability is present among ICOS and non ICOS years in both ICOS (slope = 0.23, R^2 = 0.85) and PIs processing, although median (slope = -0.05, R^2 = 0.87) is close to reference line for PI processing with 2 μmol CO_2m^{-2} s^{-1} MAE in both. Due to a change in setup, ICOS processing for ICOS and non ICOS years is not consistent, but this difference is not visible in PI processing. Both processing schemes were almost consistent for the years with only non ICOS setup with 7 % and 9 % of difference and R^2 of 0.89 for both processing. Range of variability present with the years of non ICOS setups are identical for both processing schemes with value of MAE 1.5 µmol CO_2m^{-2} s^{-1} and 1.3 µmol CO_2m^{-2} s^{-1} respectively. Likewise, years of non ICOS setup, same variability is found for years of ICOS setup with ICOS processing where median of slope is -0.09 and R^2 is 0.86 (MAE = 1.6 µmol CO_2m^{-2} s^{-1}).

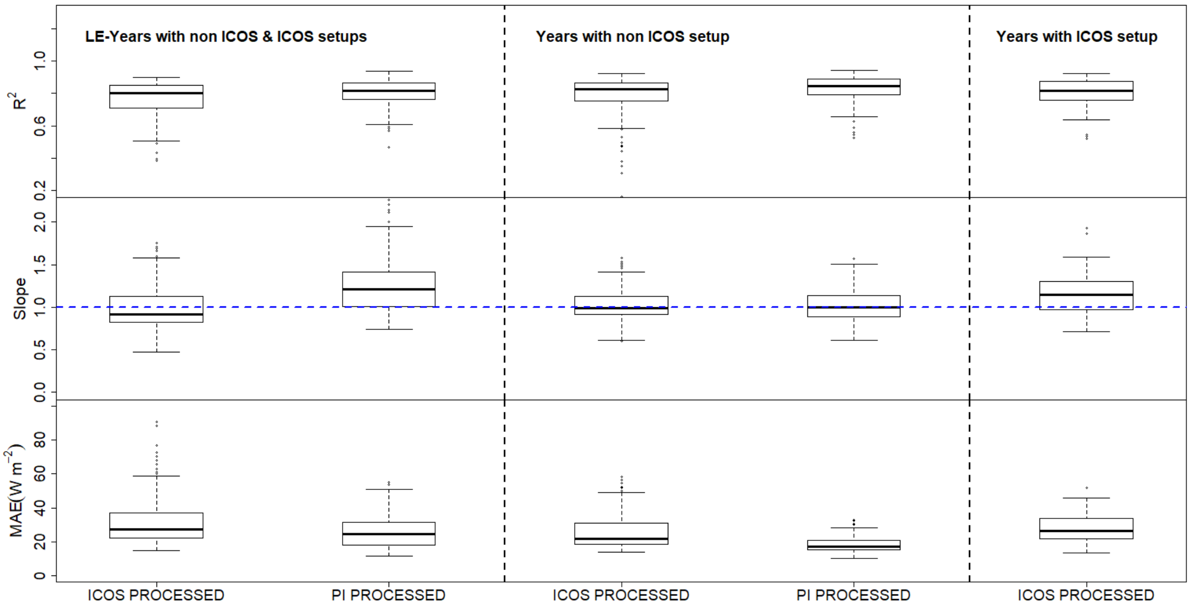

Figure 27 Box plots indicates range of R^2, slope and MAE for LE flux. R^2 and slope obtained from RMA regression analysis of fluxes between (left to right) panel 1: all the years of non ICOS setup vs ICOS setup processed by ICOS and PIs, panel 2: all the years of non ICOS setup processed by ICOS and PIs and panel 3: all the years of ICOS setup. The mark inside the box indicates the median, the edges are upper and lower quartiles. Dots represents the outliers. Blue dashed line is the 1:1 reference (slope=1).

Effect of ICOS processing and interannual variability due to ICOS processing as related to PIs processing for LE flux and H are summarized in **figure 27 and figure 28**. The plots have been constructed like in the Fc case of figure 26. Both fluxes produced nearly identical findings as the variability in the ICOS and non ICOS years is smaller in ICOS processing with respect to PIs processing. Change of setup cause difference in fluxes in both processing, although they are in different direction. For LE flux median of the slope for ICOS processing is 0.08 with 27 W m^{-2} MAE (0.80 R^2) and for PI processing is -0.21 with 25 W m^{-2} MAE (0.82 R^2). However, ICOS and PI processing schemes for H flux have slope of -0.04 (0.75 R^2) and -0.34 (0.74 R^2). Error calculated for H flux is 29 W m^{-2} and 30 W m^{-2} correspondingly. Like Fc, both processing methods have nearly comparable interannual variability among non ICOS years for LE and H fluxes. However, variation is present in term of MAE for both LE and H fluxes with the value of 21 W m^{-2} and 17 W m^{-2} for LE flux and 32 W m^{-2} and 28 W m^{-2} for H flux in ICOS and PI processing methods.

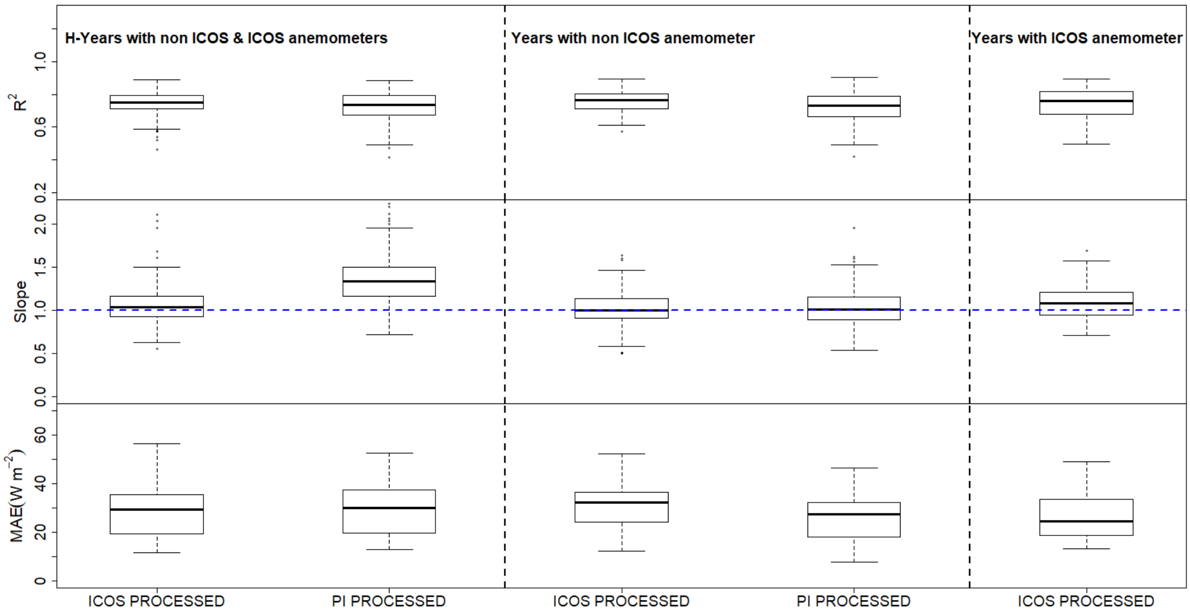

Figure 28 Box plots indicates range of R^2, slope and MAE for H flux. R^2 and slope obtained from RMA regression analysis of fluxes between (left to right) panel 1: all the years of non ICOS setup vs ICOS setup processed by ICOS and PIs, panel 2: all the years of non ICOS setup processed by ICOS and PIs and panel 3: all the years of ICOS setup. The mark inside the box indicates the median, the edges are upper and lower quartiles. Dots represents the outliers. Blue dashed line is the 1:1 reference (slope=1).

4. DISCUSSION

Eddy covariance system consists of sonic anemometer and IRGA for data acquisition to calculate fluxes. There are different models of each instrument present in the market. Use of different instrumental setups and different processing methods for calculation of fluxes introduce uncertainty that may modify the measurements. In this activity different setups and processing schemes used in eddy covariance technique are compared to evaluate their effect on calculated fluxes (CO_2, LE and H). The first section of the activity was based on the measrements obtained from parallel setups i.e. ICOS setup always consists of LI-7200 (IRGA) and HS-50 or HS-100 (sonic anemometer) and non ICOS setup that was working in parallel with ICOS setup on each site for certain time period. PIs of 15 ICOS sites shared raw EC data and their processed results for this activity. Data from parallel measurements were analyzed to evaluate: effect of 4 processing schemes (see materials and methods), effect of different setups and different processing strategies applied by ICOS and PIs of respected sites on calculated fluxes.

4.1 4 - Processing Schemes

Fc calculated from four different processing schemes proposed in ICOS do not vary much among different sites. Average of differences between Fc obtained from ICOS and non ICOS setups, calculated by 4 processing schemes ranged between 0.1 – 1 μmolCO_2 m^{-2} s^{-1}, with 0.3 μmolCO_2 m^{-2} s^{-1} difference on average The range is derived from site with smallest variation of the flux as minimum and the site with more variation as maximum. Variation in 4 processing schemes is 0.2 – 33 W m^{-2} and 1 – 24 W m^{-2} (6 and 7 W m^{-2} on average) in LE flux for ICOS and non ICOS setup and 0.3 – 5 W m^{-2} and 0.1 – 14 W m^{-2} in H flux with on average variation of 1.5 and 2 W m^{-2} for ICOS standard and other anemometers (**figures 2, 8 & 14**). Overall, in most cases there are minor variations among 4 processing schemes for Fc and H flux in case of ICOS setup with some larger difference in LE flux. From the results that are based on the median diurnal of selected data for each site emerge that variability among the fluxes processed by the 4 ICOS standard methods is smaller than the difference between the ICOS processing and the PIs processing. For this reason, it can be concluded that one out of four processing options can be used for future data processing at ICOS sites if needed, because the information added by the 4 processing on the uncertainty introduced is very small with respect to all the other sources.

4.2 Effect of Different Setups

Fluxes from two different EC setups (ICOS and non ICOS) were compared to estimate the significance of standardization of setup among different sites. Results determined that overall wide range of variability is present between the fluxes mainly Fc and LE, obtained from ICOS and non ICOS setups. This variability was also noted in the results shared by PIs of the respective sites. The differences in Fc obtained from enclosed and open path IRGA are more obvious as compared to Fc from enclosed and closed path IRGA (as fluxes from closed path and enclosed path are more consistent with each other (ICOS processing **figure 3**). Effect of different setups on all three fluxes is generally alike in terms of mean absolute error. There is small difference between the errors contributed by both processing schemes in maximum sites (**figures 3, 9 & 15**). LE flux is more complex and did not show any trend in the slopes. Likewise, Fc it is also noted that difference between the LE fluxes from enclosed path and open path IRGA type are more heterogenous in comparison with closed path IRGA type (**figure 9**).

Differences in the fluxes (Fc and LE) are mainly due the instrumental designs of closed path, open path and enclosed path IRGAs, contribution of sonic anemometer in the variation of fluxes is very small as it is observed from H flux. However, different results would be observed in winter because meteo conditions effect the sonic anemometer performances. According to the literature, closed path IRGAs have a long sampling tube, which causes attenuation of high frequency fluctuations, this affects water vapours in particular than other gases (e.g., Polonik et al., 2019). Although open path IRGAs do not have a sampling tube, precipitation and snowfall and no temperature attenuation results in a lot of data loss than substantial density corrections are required (G. Burba, 2013) that also introduce uncertainty. Maximum data loss by open path IRGA at cold environment is reported up to 90% by Goodrich et al., 2016. The enclosed path IRGA's short inlet tube boosts the attenuation of immediate temperature fluctuations while simultaneously reducing the attenuation of instantaneous water vapour fluctuations. This would effectively eliminate the WPL term (Webb et al., 1980) and associated terms, as well as the necessity for excessive frequency response corrections for water vapour flow (G. Burba et al., 2010). Random uncertainties that are stochastic nature of turbulence, instrument system, and changes in footprint also contribute variation in fluxes within same setup. In 2003, Richardson et al., concluded that random error in the flux measurement is higher for open path gas analyser than closed path analyser. Other factors e.g., missing instrument calibration of non ICOS setup, differences in the footprint sensed by the different setups, disturbances of one system to the other in the parallel periods also add minor variability in the fluxes.

H fluxes obtained from two different sonic anemometers were more comparable in both ICOS and PI processing as slopes were closer to 1, showing less variability between the H flux from two different anemometers. This is probably due to the use of one sensor for H flux (**figure 15**). The fact is also supported by Mauder and Zeeman, 2018 that H flux from CSAT, R3 and HS showed good agreement with each other. But there is variation in the average magnitude of the error in H flux obtained from different anemometer processed by different schemes. As mentioned before ICOS processing produces higher MAE in relation to PIs processing schemes. There are some sites with one IRGA working with two different anemometers or vice versa such as SE-Svb, CH-Oe2 and IT-Ren. Despite of using same IRGA or sonic anemometer, differences are observed in the fluxes. These differences are generated due to application of different processing methods and pairing of one IRGA with two different sonic anemometers or one sonic anemometer with two IRGAs also source variation in fluxes due to raw data acquisition from different logger units and distance of placememt of instruments.

4.3 Effect of Different Processing Schemes

Results pointed that Fc calculated by different processing schemes for ICOS setup are close to each other with small mean absolute error as compare to fluxes from non ICOS setup. In most of the sites (9 out of 13) ICOS processing is producing higher fluxes respect to PIs results. For non ICOS setups ICOS processing is always producing higher fluxes. Two different processing methods have relatively less impact on ICOS setup in contrast with non ICOS setup in Fc (**figure 4**). Same trend was witnessed in LE flux where majority of sites (7 out of 10) presented that flux from different processing methods was comparatively closer to each other for ICOS setup (slope and MAE). Sites where PIs applied same spectral corrections still have variabilty in fluxes due to application of different Qc methods. Differences in LE flux processed by using ICOS strategy and PIs do not show specific patterns for both ICOS and non ICOS setup. In many sites ICOS processing estimates large LE flux for both ICOS and non ICOS setups, probably because of spectral correction method applied in ICOS processing improves the estimation of LE flux **(figure 10)**. H fluxes processed by PIs and ICOS strategy do not show specific patterns for ICOS and non ICOS anemometers both for slopes and MAE. Two processing schemes have variation between fluxes but the differences observed between the slopes and MAE for ICOS and non ICOS anemometers were smaller as compared to Fc and LE flux. ICOS processing strategy overestimated H flux in comarison with PIs processing in general, due the filtering of many small or near zero flux. Howerver, spectral correction method by Fratini also has very small impact on H fluxes. Qc methods applied on the fluxes also contributed to the differences in H flux. At DE-RuS despite of different spectral correction method (Moore 1986) and Qc method (Mauder et al., 2013) used by PI, H fluxes obtained from two different anemometers agreed with each other (**figure 16**). Differences in fluxes mainly Fc and LE calculated with different processing schemes potentially associated with different spectral correction methods.

Comparison of fluxes between the calculations only (on half hours that survived after Qc filtering) disclosed that Qc filtering also contributed variability in two processing schemes. It is noted that differences between fluxes (Fc and H) obtained from different processing schemes reduced significately in maximum sites when analysis was performed on calculation of the fluxes only (**figures 5 & 17**). LE flux revealed inverse behaviour among different sites as more variation is obseved after removal of Qc filtering (**figure 12**). It is conclued that different filtering methods also contributed variability in fluxes, therefore description and documentation of these methods should be significant. Fc and LE calculated by different processing methods for ICOS setup demostrated less variation than non ICOS setup also emphasize the effect of standardization of setup (**figure 4 & 10**).

Analysis to check the percentage of data filtering only for ICOS setup validate that ICOS quality check methods, filtered more data than PIs methods. Both methods have some percentage of commom data filtering because of Foken and Wichura (1996) tests that are part of all Qc methods used by PIs. In ICOS the percentage of filtering for LE flux is more as compared to Fc and H. DE-RuS (Mauder et al., 2013) and FR-Bil (Mauder and Foken 2004) are only sites where PIs Qc methods filtered more Fc and H fluxes while, in case of LE only DE-RuS is filtering more than ICOS. Maximumum filtering for LE flux was due to EC system malfunction and abberant structural changes filtered out maximum H flux (**figures 6, 12 & 18**). The quality check in ICOS can delete up to 40% of the data, which is usually met (reference: Labelling Reports available in the ICOS Carbon Portal). This indicates that the huge percentage of data lost in the ICOS setup was due to real system issues.

4.4 Reprocessing of Long-term data

Reprocessing of long time series helped to maintain the continuity of the fluxes obtained by two different setups. 7 out of 9 sites were using closed path IRGA and ICOS processing methods include spectral correction by Fratini et al., 2012 that is a more precise correction for scalar spectral attenuation than analytic corrections. In most cases, Fc calculated using ICOS processing are lower, but they are larger in LE and H fluxes (**figures 23, 24 & 25**). Fc processed differently has significant variation among years on sites with cropland in relation to other sites. There are only two croplands so it is difficult to conclude but noticeable variation between fluxes of two processing could be due to the continuous change of flux as a result of increase in canopy height. One of two processing schemes responded more to the continuous increase in flux. Differences are quite variable between the PI processed data and ICOS processed data for non ICOS setup among sites because of application of different spectral corrections and Qc methods. Reprocessing of long-term data with ICOS processing methods helped in producing clean time series because of filtering low fluxes with ICOS Qc methods. Despite of differences in each site, the interannual variability trend is similar for both ICOS and PI processing, confirming the hypothesis that interannual trends are primarily attributable to natural and biological processes rather than artifacts caused by different setups. Interannual variation among different years on crop sites are more visible as compared to other sites, this is due to the different crop rotation among the years (**figure 23**).

Regression analysis on the 4 sites with ICOS data more than 1 year concluded significant results. It is determined that ICOS processing of non ICOS and ICOS years is not coherent for Fc. There is bias, showing that the average fluxes change when the instrument is changed. It is because ICOS processing is optimized for ICOS setup, which may result in differences when applied to non-ICOS setup. PI processing is consistent in case of Fc only whereas, change in fluxes due to change of setup is also observed in PIs processing for LE and H flux. ICOS processing of non ICOS and ICOS setup years is more comparable in LE and H probably because of application of spectral correction methods by Fratini et al., 2012. Both processing methods showed equal variability in all the fluxes for non ICOS setup (**figures 26, 27 & 28**).

CONCLUSION

The above-mentioned findings disclosed that for ICOS setup, range of variability is small among four processing schemes. One out of four options could be used for further data processing at ICOS sites. Fluxes obtained from different setups, using different methods of correction for processing of EC data have broad range of variability not only in ICOS but also PIs results. As EC is very complex method, there is not a single factor explaining the variability and differences, both the setup and the processing play a role. Fluxes obtained from ICOS and non ICOS setups working in parallel in the same ecological conditions differed from each other. On the whole it is concluded that ICOS setup has smaller variation between two different processing methods for Fc and LE flux than non ICOS setup.

Results of the activity emphasized the importance of standardization of instruments (Fc and LE flux) to reduce the variability introduced by different setups, as it is observed that differences are present not only in ICOS processed fluxes from different setups but also in PI processing of fluxes among different sites. Standardization of instruments are more significant as compared to processing methods as shown in the results that ICOS setup calculated small variation in the average magnitude of error particularly for Fc and LE flux in maximum sites. However, in case of heterogeneous setup, standardization of processing for non ICOS setups specially with closed path IRGA is very important for a correct estimation of the fluxes (mainly LE). The ICOS Qc strategy overall removed more data points and produced more efficient data cleaning, but at the same time increasing the gaps in the time series. As filtering is essential step and plays vital a role therefore, it is recommended that it should be applied on past datasets as well.

Reprocessing of long-term data by using ICOS standard processing scheme helped to reduce the effect caused by shift of instrumental setup from non ICOS to ICOS more prominently in LE and H fluxes.

The results will give the direction to follow also for other sites and in case a different setup will be decided in the context of ICOS, reducing the cross-sites variability due to choices in the processing methods and implementation. Common processing strategy should also be optimized for different setups other than ICOS. It is important that there should be proper record of metadata, timestamps, different file formats, analogue data for conversion to physical units, sensor diagnostics, maintenance, disturbance periods and processing applied for future as incomplete or missing above mentioned information could have impact on results.

REFERENCES

Aubinet, M., Clement, R., Elbers, J. A., Foken, T., Grelle, A., Ibrom, A., Moncrieff, J., Pilegaard, K., Rannik, Ü., & Rebmann, C. (2003). Methodology for data acquisition, storage, and treatment. In *Fluxes of carbon, water and energy of European Forests* (pp. 9–35). Springer.

Aubinet, M., Grelle, A., Ibrom, A., Rannik, Ü., Moncrieff, J., Foken, T., Kowalski, A. S., Martin, P. H., Berbigier, P., & Bernhofer, C. (1999). Estimates of the annual net carbon and water exchange of forests: the EUROFLUX methodology. In *Advances in ecological research* (Vol. 30, pp. 113–175). Elsevier.

Aubinet, M., Vesala, T., & Papale, D. (2012). *Eddy covariance: a practical guide to measurement and data analysis*. Springer Science & Business Media.

Baldocchi, D. (2014). Measuring fluxes of trace gases and energy between ecosystems and the atmosphere - the state and future of the eddy covariance method. *Global Change Biology*, *20*(12), 3600–3609. https://doi.org/10.1111/gcb.12649

Balzarolo, M., Boussetta, S., Balsamo, G., Beljaars, A., Maignan, F., Calvet, J.-C., Lafont, S., Barbu, A., Poulter, B., & Chevallier, F. (2014). Evaluating the potential of large-scale simulations to predict carbon fluxes of terrestrial ecosystems over a European Eddy Covariance network. *Biogeosciences*, *11*(10), 2661–2678.

Beringer, J., Hutley, L. B., McHugh, I., Arndt, S. K., Campbell, D., Cleugh, H. A., Cleverly, J., Resco de Dios, V., Eamus, D., & Evans, B. (2016). An introduction to the Australian and New Zealand flux tower network–OzFlux. *Biogeosciences*, *13*(21), 5895–5916.

Besnard, S., Carvalhais, N., Arain, M. A., Black, A., De Bruin, S., Buchmann, N., Cescatti, A., Chen, J., Clevers, J. G. P. W., & Desai, A. R. (2018). Quantifying the effect of forest age in annual net forest carbon balance. *Environmental Research Letters*, *13*(12), 124018.

Bonan, G. B., Lawrence, P. J., Oleson, K. W., Levis, S., Jung, M., Reichstein, M., Lawrence, D. M., & Swenson, S. C. (2011). Improving canopy processes in the Community Land Model version 4 (CLM4) using global flux fields empirically inferred from FLUXNET data. *Journal of Geophysical Research: Biogeosciences*, *116*(G2).

Burba, G. (2013). *Eddy Covariance Method*.

Burba, G. G., Mcdermitt, D. K., Anderson, D. J., Furtaw, M. D., & Eckles, R. D. (2010). Novel design of an enclosed CO2/H2O gas analyser for eddy covariance flux measurements. *Tellus, Series B: Chemical and Physical Meteorology*, *62*(5), 743–748. https://doi.org/10.1111/j.1600-0889.2010.00468.x

Dolman, A. J., Noilhan, J., Durand, P., Sarrat, C., Brut, A., Piguet, B., Butet, A., Jarosz, N., Brunet, Y., & Loustau, D. (2006). The CarboEurope regional experiment strategy. *Bulletin of the American Meteorological Society*, *87*(10), 1367–1380.

Eugster, W., & Senn, W. (1995). A cospectral correction model for measurement of turbulent NO2 flux. *Boundary-Layer Meteorology*, *74*(4), 321–340. https://doi.org/10.1007/BF00712375

Finkelstein, P. L., & Sims, P. F. (2001). Sampling error in eddy correlation flux measurements. *Journal of Geophysical Research: Atmospheres*, *106*(D4), 3503–3509.

Finnigan, J. J., Clement, R., Malhi, Y., Leuning, R., & Cleugh, H. A. (2003). A re-evaluation of long-term flux measurement techniques part I: averaging and coordinate rotation. *Boundary-Layer Meteorology*, *107*(1), 1–48.

Foken, Th., & Wichura, B. (1996). Tools for quality assessment of surface-based flux measurements. *Agricultural and Forest Meteorology*, *78*(1), 83–105. https://doi.org/https://doi.org/10.1016/0168-1923(95)02248-1

Foken, Thomas, Leuning, R., Oncley, S., Mauder, M., & Aubinet, M. (2012). Corrections and Data Quality Control. In *Eddy Covariance: A Practical Guide to Measurement and Data Analysis* (pp. 85–131). https://doi.org/10.1007/978-94-007-2351-1_4

Fratini, G., Ibrom, A., Arriga, N., Burba, G., & Papale, D. (2012). Relative humidity effects on water vapour fluxes measured with closed-path eddy-covariance systems with short sampling lines. *Agricultural and Forest Meteorology*, *165*, 53–63. https://doi.org/10.1016/j.agrformet.2012.05.018

Friend, A. D., Arneth, A., Kiang, N. Y., Lomas, M., Ogee, J., Rödenbeck, C., Running, S. W., SANTAREN, J., Sitch, S., & Viovy, N. (2007). FLUXNET and modelling the global carbon cycle. *Global Change Biology*, *13*(3), 610–633.

Gash, J. H. C., & Culf, A. D. (1996). Applying a linear detrend to eddy correlation data in realtime. *Boundary-Layer Meteorology*, *79*(3), 301–306. https://doi.org/10.1007/BF00119443

Göckede, M., Foken, T., Aubinet, M., Aurela, M., Banza, J., Bernhofer, C., Bonnefond, J. M., Brunet, Y., Carrara, A., Clement, R., Dellwik, E., Elbers, J., Eugster, W., Fuhrer, J., Granier, A., Grünwald, T., Heinesch, B., Janssens, I. A., Knohl, A., … Yakir, D. (2008). Quality control of CarboEurope flux data – Part 1: Coupling footprint analyses with flux data quality assessment to evaluate sites in forest ecosystems. *Biogeosciences*, *5*(2), 433–450. https://doi.org/10.5194/bg-5-433-2008

Goodrich, J. P., Oechel, W. C., Gioli, B., Moreaux, V., Murphy, P. C., Burba, G., & Zona, D. (2016). Impact of different eddy covariance sensors, site set-up, and maintenance on the annual balance of CO2and CH4in the harsh Arctic environment. *Agricultural and Forest Meteorology*, *228–229*, 239–251. https://doi.org/10.1016/j.agrformet.2016.07.008

Ibrom, A., Dellwik, E., Flyvbjerg, H., Jensen, N., & Pilegaard, K. (2007). Strong low-pass filtering effects on water vapour flux measurements with closed-path eddy correlation systems. *Agricultural and Forest Meteorology*, *147*, 140–156. https://doi.org/10.1016/j.agrformet.2007.07.007

Jung, M., Schwalm, C., Migliavacca, M., Walther, S., Camps-Valls, G., Koirala, S., Anthoni, P., Besnard, S., Bodesheim, P., & Carvalhais, N. (2020). Scaling carbon fluxes from eddy covariance sites to globe: synthesis and evaluation of the FLUXCOM approach. *Biogeosciences*, *17*(5), 1343–1365.

Law, B. E., Falge, E., Gu, L., Baldocchi, D. D., Bakwin, P., Berbigier, P., Davis, K., Dolman, A. J., Falk, M., Fuentes, J. D., Goldstein, A., Granier, A., Grelle, A., Hollinger, D., Janssens, I. A., Jarvis, P., Jensen, N. O., Katul, G., Mahli, Y., … Wofsy, S. (2002). Environmental controls over carbon dioxide and water vapor exchange of terrestrial vegetation. *Agricultural and Forest Meteorology*, *113*(1–4), 97–120. https://doi.org/10.1016/S0168-1923(02)00104-1

Loescher, H. W., Law, B. E., Mahrt, L., Hollinger, D. Y., Campbell, J., & Wofsy, S. C. (2006). Uncertainties in, and interpretation of, carbon flux estimates using the eddy covariance technique. *Journal of Geophysical Research Atmospheres*, *111*(21), 1–19. https://doi.org/10.1029/2005JD006932

Luyssaert, S., Inglima, I., Jung, M., Richardson, A. D., Reichstein, M., Papale, D., Piao, S. L., Schulze, E., Wingate, L., & Matteucci, G. (2007). CO2 balance of boreal, temperate, and tropical forests derived from a global database. *Global Change Biology*, *13*(12), 2509–2537.

Mahecha, M. D., Reichstein, M., Carvalhais, N., Lasslop, G., Lange, H., Seneviratne, S. I., Vargas, R., Ammann, C., Arain, M. A., & Cescatti, A. (2010). Global convergence in the temperature sensitivity of respiration at ecosystem level. *Science*, *329*(5993), 838–840.

Mammarella, I., Launiainen, S., Gronholm, T., Keronen, P., Pumpanen, J., Rannik, Ü., & Vesala, T. (2009). Relative humidity effect on the high-frequency attenuation of water vapor flux measured by a closed-path eddy covariance system. *Journal of Atmospheric* *and Oceanic Technology*, *26*(9), 1856–1866. https://doi.org/10.1175/2009JTECHA1179.1

Mammarella, I., Peltola, O., Nordbo, A., & Järvi, L. (2016). Quantifying the uncertainty of eddy covariance fluxes due to the use of different software packages and combinations of processing steps in two contrasting ecosystems. *Atmospheric Measurement Techniques*, *9*(10), 4915–4933. https://doi.org/10.5194/amt-9-4915-2016

Mauder, M., Cuntz, M., Drüe, C., Graf, A., Rebmann, C., Schmid, H. P., Schmidt, M., & Steinbrecher, R. (2013). A strategy for quality and uncertainty assessment of long-term eddy-covariance measurements. *Agricultural and Forest Meteorology*, *169*, 122–135. https://doi.org/https://doi.org/10.1016/j.agrformet.2012.09.006

Mauder, M., & Foken, T. (2006). Impact of post-field data processing on eddy covariance flux estimates and energy balance closure. *Meteorologische Zeitschrift*, *15*, 597–609. https://doi.org/10.1127/0941-2948/2006/0167

Mauder, M., & Zeeman, M. J. (2018). Field intercomparison of prevailing sonic anemometers. *Atmospheric Measurement Techniques*, *11*(1), 249–263. https://doi.org/10.5194/amt-11-249-2018

Moncrieff, J. B., Massheder, J. M., de Bruin, H., Elbers, J., Friborg, T., Heusinkveld, B., Kabat, P., Scott, S., Soegaard, H., & Verhoef, A. (1997). A system to measure surface fluxes of momentum, sensible heat, water vapour and carbon dioxide. *Journal of Hydrology*, *188–189*, 589–611. https://doi.org/https://doi.org/10.1016/S0022-1694(96)03194-0

Novick, K. A., Biederman, J. A., Desai, A. R., Litvak, M. E., Moore, D. J. P., Scott, R. L., & Torn, M. S. (2018). The AmeriFlux network: A coalition of the willing. *Agricultural and Forest Meteorology*, *249*, 444–456.

Papale, D. (2020). Ideas and perspectives: enhancing the impact of the FLUXNET network of eddy covariance sites. *Biogeosciences*, *17*(22), 5587–5598. https://doi.org/10.5194/bg-17-5587-2020

Papale, D., Mammarella, I., & Sabbatini, S. (2016). *Protocol on Processing of Eddy Covariance Raw Data – ICOS Version : 20150302*. *20150302*, 1–22.

Polonik, P., Chan, W. S., Billesbach, D. P., Burba, G., Li, J., Nottrott, A., Bogoev, I., Conrad, B., Biraud, S. C., & Berkeley, L. (2019). *Agricultural and Forest Meteorology Comparison of gas analyzers for eddy covariance : Effects of analyzer type and spectral corrections on fluxes*. *273*(February), 128–142. https://doi.org/10.1016/j.agrformet.2019.02.010

Rannik, Ü., & Vesala, T. (1999). Autoregressive filtering versus linear detrending in estimation of fluxes by the eddy covariance method. *Boundary-Layer Meteorology*, *91*(2), 259–280. https://doi.org/10.1023/A:1001840416858

Rebmann, C., Kolle, O., Heinesch, B., Queck, R., Ibrom, A., & Aubinet, M. (2012). Eddy Covariance. *Eddy Covariance*. https://doi.org/10.1007/978-94-007-2351-1

Reichstein, M., Papale, D., Valentini, R., Aubinet, M., Bernhofer, C., Knohl, A., Laurila, T., Lindroth, A., Moors, E., & Pilegaard, K. (2007). Determinants of terrestrial ecosystem carbon balance inferred from European eddy covariance flux sites. *Geophysical Research Letters*, *34*(1).

Restrepo-Coupe, N., da Rocha, H. R., Hutyra, L. R., da Araujo, A. C., Borma, L. S., Christoffersen, B., Cabral, O. M. R., de Camargo, P. B., Cardoso, F. L., da Costa, A. C. L., Fitzjarrald, D. R., Goulden, M. L., Kruijt, B., Maia, J. M. F., Malhi, Y. S., Manzi, A. O., Miller, S. D., Nobre, A. D., von Randow, C., … Saleska, S. R. (2013). What drives the seasonality of photosynthesis across the Amazon basin? A cross-site analysis of eddy flux tower measurements from the Brasil flux network. *Agricultural and Forest Meteorology*, *182–183*, 128–144. https://doi.org/10.1016/j.agrformet.2013.04.031

Richardson, A. D., Aubinet, M., Barr, A. G., Hollinger, D. Y., Ibrom, A., Lasslop, G., & Reichstein, M. (2012). Uncertainty quantification. In *Eddy covariance* (pp. 173–209). Springer.

Richardson, A. D., Hollinger, D. Y., Burba, G. G., Davis, K. J., Flanagan, L. B., Katul, G. G., William Munger, J., Ricciuto, D. M., Stoy, P. C., Suyker, A. E., Verma, S. B., & Wofsy, S. C. (2006). A multi-site analysis of random error in tower-based measurements of carbon and energy fluxes. *Agricultural and Forest Meteorology*, *136*(1–2), 1–18. https://doi.org/10.1016/j.agrformet.2006.01.007

Sabbatini, S., Mammarella, I., Arriga, N., Fratini, G., Graf, A., Hörtnagl, L., Ibrom, A., Longdoz, B., Mauder, M., Merbold, L., Metzger, S., Montagnani, L., Pitacco, A., Rebmann, C., Sedlák, P., Šigut, L., Vitale, D., & Papale, D. (2018). Eddy covariance raw data processing for CO 2 and energy fluxes calculation at ICOS ecosystem stations. *International Agrophysics*, *32*(4), 495–515. https://doi.org/10.1515/intag-2017-0043

Schotanus, P., Nieuwstadt, Ftm., & De Bruin, H. A. R. (1983). Temperature measurement with a sonic anemometer and its application to heat and moisture fluxes. *Boundary-Layer Meteorology*, *26*(1), 81–93.

Taylor, J. R., & Loescher, H. L. (2013). Automated quality control methods for sensor data: a novel observatory approach. *Biogeosciences*, *10*(7), 4957–4971.

Van Dijk, A., Moene, A. F., & De Bruin, H. A. R. (2004). The principles of surface flux physics: theory, practice and description of the ECPACK library. *Meteorology and Air Quality Group, Wageningen University, Wageningen, the Netherlands*, *99*, 525.

Vickers, D., & Mahrt, L. (1997). Quality control and flux sampling problems for tower and aircraft data. *Journal of Atmospheric and Oceanic Technology*, *14*(3), 512–526.

Vitale, D., Fratini, G., Bilancia, M., Nicolini, G., Sabbatini, S., & Papale, D. (2020). A robust data cleaning procedure for eddy covariance flux measurements. *Biogeosciences*, *17*(6), 1367–1391. https://doi.org/10.5194/bg-17-1367-2020

Webb, E. K., Pearman, G. I., & Leuning, R. (1980). Correction of flux measurements for density effects due to heat and water vapour transfer. *Quarterly Journal of the Royal MeteorologicalSociety*, *106*(447), 85–100.

Wilczak, J. M., Oncley, S. P., & Stage, S. A. (2001). Sonic anemometer tilt correction algorithms. *Boundary-Layer Meteorology*, *99*(1), 127–150.

Williams, M., Richardson, A. D., Reichstein, M., Stoy, P. C., Peylin, P., Verbeeck, H., Carvalhais, N., Jung, M., Hollinger, D. Y., & Kattge, J. (2009). Improving land surface models with FLUXNET data. *Biogeosciences*, *6*(7), 1341–1359.

Yamamoto, S., Saigusa, N., Gamo, M., Fujinuma, Y., Inoue, G., & Hirano, T. (2005). Findings through the AsiaFlux network and a view toward the future. *Journal of Geographical Sciences*, *15*(2), 142–148.

Yu, G.-R., Wen, X.-F., Sun, X.-M., Tanner, B. D., Lee, X., & Chen, J.-Y. (2006). Overview of ChinaFLUX and evaluation of its eddy covariance measurement. *Agricultural and Forest Meteorology*, *137*(3–4), 125–137.

APPENDICES

Percentages of data available for each flux in the tables are calculated from MDC of 6*48 from all the site. Total number of half hours were 288.

Sites	DB_non-ICOS	DB_ICOS	DL_non-ICOS	DL_ICOS	PB_non-ICOS	PB_ICOS	PL_non-ICOS	PL_ICOS	non_ICOS_PI	ICOS_PI
DE-Geb	100	100	100	100	100	100	100	100	100	100
DE-Tha	100	100	100	100	100	100	100	100	100	100
CZ-Bk1	100	100	100	100	100	100	100	100	100	100
BE-Lon	92	100	92	100	92	100	88	100	90	100
FR Pue*	7	83	7	83	7	83	7	83	100	83
FR-Bil	100	100	100	100	100	100	100	100	100	100
FR-Fon*	36	100	39	100	36	100	38	100	100	100
CZ-Wet	98	99	98	99	98	99	98	99	89	98
FR-Aur	99	100	99	100	99	100	99	100	100	100
FR-Lam	100	100	100	100	52	100	51	100	100	100
DE-RuS	100	100	100	100	100	100	100	100	83	83
CH-Oe2	94	97	94	97	94	97	95	97	100	100
IT-Ren	96	96	96	95	96	95	96	95	100	100
IT-Mbo	96	100	96	100	96	100	96	100	100	100
SE-Svb	100	100	100	100	100	100	100	100	100	100

Table 1 Percentages of data available for Fc flux obtained from ICOS and non ICOS setups, processed by ICOS and PIs from different sites. DB = double rotaion and block average, DL= double rotation and linear detrending, PB = planar fit and block average and PL = planar fit and linear detrending (4 processing schemes for ICOS and non ICOS setup) non_ICOS_PI = PIs results from non ICOS setup and ICOS_ PI = PIs results from ICOS setup. Sites with * were excluded from analysis.

Sites	DB_non-ICOS	DB_ICOS	DL_non-ICOS	DL_ICOS	PB_non-ICOS	PB_ICOS	PL_non-ICOS	PL_ICOS	non_ICOS_PI	ICOS_PI
DE-Geb	100	99	100	99	100	99	100	99	100	100
DE-Tha	99	100	99	100	99	100	99	100	100	100
CZ-Bk1	100	100	100	100	100	100	100	100	100	100
BE-Lon*	100	100	100	100	100	100	92	100	0	100
FR-Pue*	36	82	36	82	36	82	36	82	100	83
FR-Bil	94	91	94	91	94	91	94	91	100	100
FR-Fon*	39	100	55	100	39	97	41	97	100	100
CZ-Wet	90	68	90	68	90	67	90	68	99	99
FR-Aur	99	89	99	89	99	89	99	89	100	100
FR-Lam*	20	57	20	57	20	56	20	56	100	100
DE-RuS	100	100	100	100	100	100	100	100	83	83
CH-Oe2	85	72	85	72	85	72	85	72	100	100
IT-Ren*	93	94	94	94	94	94	94	94	100	100
IT-Mbo	98	99	98	99	98	99	98	99	100	100
SE-Svb	100	100	100	100	100	100	100	100	100	100

Table 2 Percentages of data available for LE flux obtained from ICOS and non ICOS setups, processed by ICOS and PIs from different sites. DB = double rotaion and block average, DL= double rotation and linear detrending, PB = planar fit and block average and PL = planar fit and linear detrending (4 processing schemes for ICOS and non ICOS setup) non_ICOS_PI = PIs results from non ICOS setup and ICOS_ PI = PIs results from ICOS setup. Sites with * were excluded from analysis. IT-Ren was not included due to problem that was more noticeable in LE.

Sites	DB_non-ICOS	DB_ICOS	DL_non-ICOS	DL_ICOS	PB_non-ICOS	PB_ICOS	PL_non-ICOS	PL_ICOS	non_ICOS_PI	ICOS_PI
DE-Geb	99	100	99	100	99	100	99	100	100	100
DE-Tha*	100	5	100	5	100	5	100	5	100	100
CZ-Bk1	100	100	100	100	100	100	100	100	100	100
BE-Lon	99	100	99	100	99	100	95	100	100	100
FR-Pue	100	100	100	100	100	100	100	100	100	100
FR-Bil	100	100	100	100	100	100	100	100	100	100
FR-Fon	100	100	100	100	100	100	100	100	100	100
CZ-Wet	100	98	99	98	100	98	99	98	100	100
FR-Aur	100	100	100	100	100	100	100	100	100	100
FR-Lam	83	100	83	100	80	100	80	100	83	100
DE-RuS	100	100	100	100	100	100	100	99	83	83
CH-Oe2	100	99	100	99	100	99	100	99	100	100
IT-Ren	99	99	100	100	99	99	99	99	100	100
IT-Mbo*	12	100	12	100	12	100	12	100	100	100
SE-Svb	100	100	100	100	100	100	100	100	100	100

Table 3 Percentages of data available for H flux obtained from ICOS and non ICOS setups, processed by ICOS and PIs from different sites. DB = double rotaion and block average, DL= double rotation and linear detrending, PB = planar fit and block average and PL = planar fit and linear detrending (4 processing schemes for ICOS and non ICOS setup) non_ICOS_PI = PIs results from non ICOS setup and ICOS_ PI = PIs results from ICOS setup. Sites with * were excluded from analysis.

YEARS	Fc_ICOS	Fc_PI	LE_ ICOS	LE_PI	H_ ICOS	H_PI
2002	80	100	77	100	82	100
2003	81	100	47	100	60	100
2004	89	100	81	100	93	100
2005	72	100	66	100	66	100
2006	79	100	66	100	66	100
2007	89	100	70	100	70	100
2008	94	100	84	100	64	100
2009	64	100	58	100	63	100
2010	78	100	53	100	93	100
2011	90	100	78	100	81	100
2012	74	100	61	100	94	100
2013	100	100	88	100	95	100
2014	95	100	84	100	94	100
2015	97	100	92	100	100	100
2016	97	100	76	100	93	100
2017	100	-	99	-	100	-

Table 4 Percentages of long-term data available for Fc, LE and H flux in ICOS and PI processing at DE-Geb.

YEARS	Fc_ICOS	Fc_PI	LE_ ICOS	LE_PI	H_ ICOS	H_PI
2001	100	100	100	100	100	100
2002	80	67	68	67	83	100
2003	99	100	95	100	100	100
2004	100	100	100	100	100	100
2005	100	100	100	100	100	100
2006	100	100	100	100	100	100
2007	100	100	100	100	100	100
2008	100	100	100	100	100	100
2009	100	100	100	100	100	100
2010	100	100	100	100	100	100
2011	100	100	100	100	100	100
2012	100	100	100	100	100	100
2013	100	100	100	100	100	100
2014	100	100	90	100	100	100
2015	100	100	100	100	100	100
2016	100	100	99	100	100	100
2017	100	-	100	-	5	-

Table 5 Percentages of long-term data available for Fc, LE and H flux in ICOS and PI processing at DE-Tha.

YEARS	Fc_ICOS	Fc_PI	LE_ ICOS	LE_PI	H_ ICOS	H_PI
2006	100	100	99.3	100	100	100
2007	99.7	100	84.7	100	99.7	100
2008	100	100	100	100	100	100
2009	100	100	100	100	100	100
2010	100	100	99.7	100	100	100
2011	100	100	100	100	100	100
2012	100	-	100	-	100	-
2013	50	-	50	-	100	-
2014	100	-	100	-	100	-
2015	100	-	100	-	100	-
2016	100	-	100	-	100	-
2017	100	-	100	-	100	-
2018	100	-	100	-	100	-

Table 6 Percentages of long-term data available for Fc, LE and H flux in ICOS and PI processing at CZ-BK1.

YEARS	Fc_ICOS	Fc_PI	LE_ ICOS	LE_PI	H_ ICOS	H_PI
2006	100	100	97	100	99	100
2007	100	100	99	100	97	100
2008	100	100	99	100	98	100
2009	100	100	98	100	97	100
2010	100	100	99	100	99	100
2011	100	100	97	100	98	100
2012	100	100	98	100	98	100
2013	100	100	99	100	95	100
2014	100	-	100	-	100	-

Table 7 Percentages of long-term data available for Fc, LE and H flux in ICOS and PI processing at BE-Lon.

YEARS	Fc_ICOS	Fc_PI	LE_ ICOS	LE_PI	H_ ICOS	H_PI
2001	100	100	99.7	100	100	100
2002	100	100	100	100	100	100
2003	100	100	99.3	100	100	100
2004	100	100	100	100	100	100
2005	100	100	99.7	100	100	100
2006	99.7	100	99.3	100	100	100
2007	100	100	98.6	100	100	100
2008	100	100	99.7	100	100	100
2009	100	100	99.7	100	100	100
2010	100	100	99.3	100	100	100
2011	100	100	98.6	100	95.5	96.2
2012	85.8	100	98.6	100	100	100
2013	97.9	100	99	100	99.7	100
2014	99.7	-	99.7	-	100	-

Table 8 Percentages of long-term data available for Fc, LE and H flux in ICOS and PI processing at FR-Pue.

YEARS	Fc_ICOS	Fc_PI	LE_ ICOS	LE_PI	H_ ICOS	H_PI
2001	100	100	97	100	99	100
2002	100	100	100	100	100	100
2003	100	100	92	100	100	100
2004	100	100	100	100	100	100
2005	100	100	100	100	100	100
2006	100	100	100	100	100	100
2007	100	100	100	100	100	100
2008	100	100	100	100	100	100
2009	100	100	100	100	100	100
2010	100	100	97	100	100	100
2011	100	100	100	100	100	100
2012	100	100	100	100	100	100
2013	100	100	100	100	100	100
2014	100	100	100	100	100	100
2015	100	100	100	100	100	100
2016	100	100	100	100	100	100
2017	100	100	100	100	100	100
2018	100	-	100	-	100	-
2019	100	-	100	-	100	-
2020	100	-	100	-	100	-

Table 9 Percentages of long-term data available for Fc, LE and H flux in ICOS and PI processing at FI-Hyy.

YEARS	Fc_ICOS	Fc_PI	LE_ ICOS	LE_PI	H_ ICOS	H_PI
2005	100	100	100	100	100	100
2006	66.3	66.7	66.3	66.7	66.3	66.7
2007	100	100	99.3	100	100	100
2008	99.7	100	100	100	100	100
2009	60.8	60.1	68.8	60.1	100	100
2010	100	100	99.3	100	100	100
2011	99.7	100	84.4	100	99.3	100
2012	100	100	100	100	99.7	100
2013	100	100	100	100	100	100
2014	50	50	50	50	100	100
2015	100	-	100	-	100	-
2016	100	-	100	-	99.7	-
2017	99.3	-	99.7	-	99.3	-
2018	92.7	-	96.2	-	95.8	-
2019	99.7	-	100	-	100	-
2020	100	-	100	-	100	-

Table 10 Percentages of long-term data available for Fc, LE and H flux in ICOS and PI processing at FI-Sii.

YEARS	Fc_ICOS	Fc_PI	LE_ ICOS	LE_PI	H_ ICOS	H_PI
2006	88.9	86.8	82.3	89.9	87.5	95.1
2007	28.1	99.3	33.3	100	0.0	100
2008	100	97.9	93.4	100	99.7	100
2009	99.3	98.6	60.4	100	100	100
2010	99	96.9	85.8	99.3	100	100
2011	99	97.6	95.5	100	100	100
2012	100	-	94.8	-	100	-
2013	100	-	93.8	-	100	-
2014	100	-	89.2	-	100	-
2015	100	-	97.2	-	99.7	-
2016	100	-	93.8	-	100	-
2017	98.6	-	99.7	-	95.5	-

Table 11 Percentages of long-term data available for Fc, LE and H flux in ICOS and PI processing at CZ-Wet.

YEARS	Fc_ICOS	Fc_PI	LE_ ICOS	LE_PI	H_ ICOS	H_PI
2014	60.8	83.3	0.3	83.3	76.7	50
2015	100	100	90.6	100	100	100
2016	100	-	71.5	-	100	-
2017	100	-	81.9	-	100	-
2018	99	-	96.9	-	96.9	-
2019	0	-	0	-	0	-
2020	100	-	100	-	100	-

Table 12 Percentages of data available for Fc, LE and H flux in ICOS and PI processing at FR-Bil.